Exciton dynamics in α-particle tracks in organic crystals: Magnetic field study of the scintillation in tetracene crystals

Nicholas E. Geacintov, Michael Binder, Charles E. Swenberg, and Martin Pope
Radiation and Solid State Laboratory and Chemistry Department, New York University, New York, New York 10003
(Received 13 January 1975)

The mechanisms of scintillation of organic crystals bombarded by α particles are discussed in terms of the current knowledge of exciton dynamics, which has been derived from a study of the photofluorescence of crystals such as anthracene and tetracene. The scintillation of tetracene excited by 4.4-MeV α particles incident in a direction perpendicular to the *ab* plane has been studied in the presence of external magnetic fields (0–4000 G) and compared to the scintillation of crystalline anthracene. At 298 °K, the magnetic field effect on the total scintillation yield is $(+2.5 \pm 0.5)\%$ in tetracene and displays a typical fissionlike (fission of one singlet exciton into two triplets) dependence. At low temperatures when fission is suppressed, a fusionlike dependence (reverse of fission) appears with a $(-4$ to $-5)\%$ effect at 4000 G at 148 °K. In anthracene, the fusionlike dependence is observed at all temperatures in the range studied (148–298 °K). Using appropriate kinetic equations, expressions are derived for the prompt (L_P) and delayed (L_D) components of the total scintillation yield $L = L_P + L_D$. These expressions describe the temperature and magnetic field dependence of L, which arises because of the temperature and magnetic field dependence of the exciton fission and fusion rate constants in tetracene. In tetracene, L_D appears to be strongly temperature dependent, while L_P is not. This is explained in terms of the high density of transient singlet exciton quenchers in the α-particle track. The density of these transient quenchers is estimated to be in the range of 3×10^{17}–5×10^{18} cm^{-3}, and they are identified, in accord with a previous suggestion by Schott, as triplet excitons which are created by random recombination of electrons and holes in the α-particle track. The delayed scintillation L_D which arises from the fusion of two triplet excitons is proportional to $\gamma_{rad}/\gamma_{tot}$ (where γ_{rad} is the radiative and γ_{tot} the total rate constant for the fusion of two triplets), whereas under conditions of weak photoexcitation, the delayed fluorescence is proportional to γ_{rad}. It is shown how the contribution of L_D to L can be estimated from the magnetic field dependence of L. In tetracene, this contribution of the delayed component is $\sim$10% at 298°K, and $\sim$50% at 150°K. whereas in anthracene the contribution of L_D is $\sim(50$–$70)\%$. The ratio of the L values for anthracene/tetracene was found to be 6 ± 2 at 298°K and to be of the order of unity at 148°. This is in contrast to the photofluorescence efficiency which at 298 °K is 50 to 100 times lower in tetracene because of fission. This behavior is attributed to a lack of a temperature dependence of L_P in tetracene because this quenching of singlets by triplets dominates over the fission term (the singlet exciton lifetime in the α-particle track is estimated to be about 10^{-11} sec in tetracene). Irradiation of tetracene for prolonged periods of time (equivalent to a dose of 10^6 rad) changes the magnetic field dependence at room temperature from the small positive fissionlike dependence to a negative (-2%) fusionlike dependence. This is due to the introduction of permanent singlet exciton quenching centers which effectively compete with fission and whose density is estimated to be of the order of 10^{18} cm^{-3}.

INTRODUCTION

The scintillation produced by the passage of an energetic particle in organic crystals has been widely studied within the last twenty years. The earlier work has been summarized by Birks.[1] Anthracene is one of the best characterized materials; its scintillation response L to different ionizing particles of various energies E have been studied by many workers. For fast electrons with $E \gtrsim 125$ keV, the specific luminescence dL/dx (mean number of photons emitted per unit path length of the electrons) is proportional to the specific energy loss (or stopping power) dE/dx. For slow electrons ($E < 125$ keV) and for heavier particles, such as α particles, the specific luminescence for the same dE/dx is considerably lower than for fast electrons. This effect has been attributed to the quenching of fluorescence-emitting singlet excitons by the high density of ionized and other excited states which are produced along the α-particle or slow-electron tracks; fast electrons produce only a weak excitation and ionization density along their path within the crystal. Since dE/dx is relatively low, the quenching centers are spaced relatively far apart from each other and from the singlet excitons, and the quenching of the latter is thus minimal. With α particles the magnitude of the quenching within the track is much higher than the quenching produced by *permanent* (long-lived) quenchers which are produced by radiation damage. According to Birks,[1] most of the quenching within a heavy-particle (or slow-electron) track is produced by *transient* quenching centers which have a lifetime

of the order of the main scintillation emission decay time, which is several nanoseconds or less. These transient quenching centers are assumed to be temporarily ionized or excited molecules.[1] Semiempirical relationships were proposed to account for this ionization quenching by Birks[2] and by Wright.[3] More recently an improved theoretical relationship between dL/dx and dE/dx was derived by Voltz and his co-workers.[4] Their relation takes into account the fact that the scintillation consists of two components: a slow (delayed) component due to triplet-triplet annihilation[5] (or exciton fusion) and a fast (prompt) component which is due to a direct excitation of singlet states by the primary particle or by secondary electrons (δ rays).

Extensive studies on the scintillation of α-particle-bombarded organic crystals, primarily anthracene, have shown that the scintillation response of anthracene (and of other crystals) depends on the direction of the α-particle beam with respect to the crystallographic axes.[6,7] Attempts have been made to explain this effect in terms of anisotropic exciton diffusion,[6] anisotropic thermal quenching,[8] and more recently[9,10] in terms of the equations of Voltz *et al.*[4]

The basic ideas of the mechanisms of scintillation in organic crystals were discussed by Birks,[1] by Voltz,[11] and most recently by Schott.[12] Basically, the scintillation is produced by the decay of singlet excitons. The latter can be formed by either or all of the following processes: (i) Decay of superexcited states, (ii) electron-hole recombination within the tracks, where the electrons and holes are formed from autoionization of superexcited states, or (iii) triplet-triplet exciton annihilation (fusion) which gives rise to the delayed component of the scintillation.[5] The triplet excitons can, in principle, be formed by electron-hole recombination or by intersystem crossover from singlet excitons.

The singlet excitons S_1 can decay via the emission of a fluorescence photon, by self-quenching (singlet-singlet annihilation), or by quenching owing to electrons, holes, free radicals, or triplet excitons[12] within the track. The efficiency of these processes depends strongly on the concentration of the quenching species $[Q]$ and on the interaction rate constant γ between S_1 and Q. If the concentration of the latter within the α-particle track decreases with time because of diffusion, or various decay mechanisms, these quenchers are "transient" rather than "permanent" and can account for the magnitude of the observed ionization quenching.[12]

Within the last decade significant advances have been made in understanding excitonic processes in organic crystals using ultraviolet or visible photoexcitation. The use of external magnetic fields in the range of 0–5000 G has been instrumental in elucidating the details of exciton interactions involving triplets and paramagnetic doublet states. The recent advances in exciton dynamics in general, and magnetic field effects in particular, have been summarized in reviews by Avakian and Merrifield,[13–15] by Swenberg and Geacintov,[16] and by Sokolik and Frankevich.[17]

In this work, we apply the knowledge gained from photoexcitation studies, particularly in the presence of an external magnetic field, to an analysis of scintillation phenomena in tetracene single crystals. The effect of external magnetic fields on the scintillation of anthracene single crystals bombarded by α and β particles was first observed by Klein and Voltz.[18] We had previously reported the observation of a magnetic field effect on the scintillation of tetracene crystals produced by α particles.[19] In this paper we present a detailed analysis of these effects.

We selected crystalline tetracene rather than the more widely studied anthracene for several important reasons. In tetracene an external magnetic field can produce either an enhancement or a decrease in the total fluorescence, depending on the ambient conditions. At room temperature, a fluorescence enhancement of (20–40)% is observed due to the partial blocking of a thermally stimulated and magnetic field-sensitive fission of one singlet exciton into two triplets. The triplet-exciton fusion process which leads to singlet excitons normally produces the delayed fluorescence and also has a magnetic field dependence; however, this dependence is masked at room temperature by the effect of the magnetic field on the fission of the singlet exciton that is produced by the fusion process. Below 160 °K the singlet-exciton fission is thermally suppressed[20] and the fusion[21,22] of two triplet excitons to form one singlet exciton is observed. The efficiency of this process is reduced by magnetic fields $\gtrsim 500$ G and the delayed fluorescence intensity is decreased. Therefore, because of the coexistence of fission and fusion,[22] both processes can be studied by examining the scintillation produced by α particles at different temperatures. In crystalline anthracene on the other hand, although triplet-exciton fusion is operative, thermally induced fission is absent. Owing to fission, the singlet-exciton lifetime in tetracene is only $\sim 2\times 10^{-10}$ sec[23,24] at room temperature. The magnetic field tends to decrease the fission-rate constant and thus produces an increase in the photoinduced fluorescence efficiency by as much as (20–40)%.

In addition the fluorescence efficiency depends on the external field orientation with respect to the crystallographic axis. This anisotropy dependence for magnetic fields greater than 2 kG ex-

hibits two maxima every 180° with their separation depending only on the ratio of the spin-Hamiltonian parameters and orientations of the molecules in the crystal. If the singlet excitons are quenched effectively on the time scale of $\sim 10^{-10}$ sec by processes other than fission, the magnetic field effect will be reduced (as long as the quenching process itself is not magnetic field sensitive). The magnitude of the magnetic field effect and its orientation with respect to the crystallographic axis can thus provide information on fast-quenching processes which occur in α-particle tracks and can be used to probe energy-dissipation mechanisms on time scales less than 10^{-10} sec.

This paper is divided into several sections. In Sec. I the known magnetic field effects and correlative exciton processes are reviewed with special emphasis on those phenomena which are likely to occur in α-particle tracks. In Sec. II the possible mechanisms of energy dissipation in terms of excitonic phenomena are discussed and the time scales of various processes which directly or indirectly may affect the scintillation efficiency are estimated. The basic kinetic equations for scintillation are developed in Sec. III and the experimental details are described in Sec. IV. The experimental results are analyzed in Sec. V to IX.

I. EXCITONIC PHENOMENA AND ASSOCIATED MAGNETIC FIELD EFFECTS IN CRYSTALLINE TETRACENE

An energy-level diagram of crystalline tetracene is shown in Fig. 1. The fluorescence efficiency of crystalline tetracene is only ~ 0.002,[25] and increases strongly with decreasing temperature. In contrast, the fluorescence efficiency of crystalline anthracene is close to unity.[1]

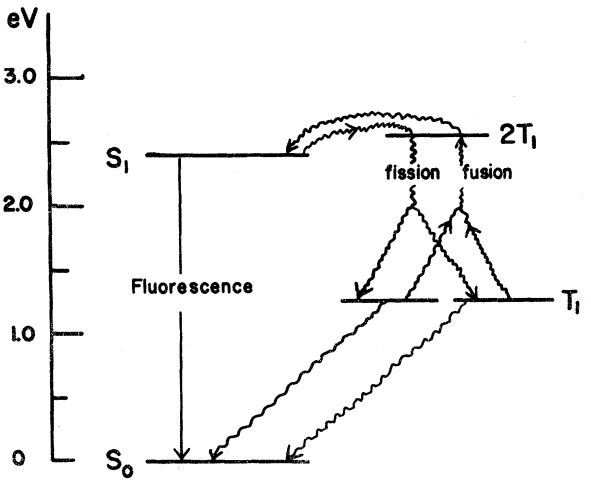

FIG. 1. Simplified energy-level diagram for tetracene. S_1, singlet exciton; T_1, triplet exciton; $2T_1$, triplet-exciton pair state energy. The exciton fission and fusion processes are indicated schematically.

A. Singlet exciton fission

At room temperature the singlet excitons (S_1) spontaneously fission into two triplet excitons (T_1) according to the scheme

$$S_0 + S_1 + \Delta E \xrightarrow{\gamma_f} T_1 + T_1 \ , \tag{1}$$

where $\Delta E = 0.21$ eV is the difference in energy between the S_1 and double triplet ($2T_1$) energy levels.[26] Fission accounts for the relatively low fluorescence efficiency in tetracene at room temperature. (In anthracene, $\Delta E = 0.51$ eV and thermally induced fission is not observed at 300 °K. However, fission of vibrationally excited levels of S_1 and upper excited-singlet states can occur with low efficiency.[27]) The fission constant is equal to

$$\gamma_f \approx 1.5 \times 10^{-12} \text{ cm}^3 \text{ sec}^{-1} \ ,$$

which corresponds to a singlet-exciton lifetime τ_s at room temperature[23,24] of

$$\tau_s = (\gamma_f [S_0])^{-1} \cong 2 \times 10^{-10} \text{ sec} \ ,$$

S_0 is the concentration of tetracene molecules in the crystal.

The coupling of the singlet-exciton with the triplet-exciton pair states in Eq. (1) is magnetic field sensitive. This is due to an interplay between the Zeeman energy and intramolecular spin-spin interaction which together are functions of both the magnetic field strength and the direction of the field with respect to the crystallographic axes. Originally this effect was explained by Merrifield[28] and is discussed in detail in the reviews cited.[14-16]

Since fission and fluorescence are competitive modes of decay of S_1, the prompt (photoexcited) fluorescence efficiency is magnetic field sensitive. Below ~ 400 G the magnetic field decreases the fluorescence F, while F is increased for fields above 400 G. The effect saturates at about 3000 G and remains constant when the magnetic field is increased further up to 100 000 G.[29] A typical field dependence of the fluorescence of tetracene at room temperature is shown in Fig. 2(a).

B. Fusion of triplet excitons

This process is represented by

$$T_1 + T_1 \xrightarrow{\gamma_{rad}} S_1 + S_0 \tag{2}$$

and leads to delayed fluorescence. The latter has a decay time which is comparable to the triplet-exciton lifetime τ_T (which lies in the range of 50–200 μsec in tetracene).[30] The magnetic field dependence of the delayed fluorescence is opposite to the one shown for fission and is displayed in Fig.

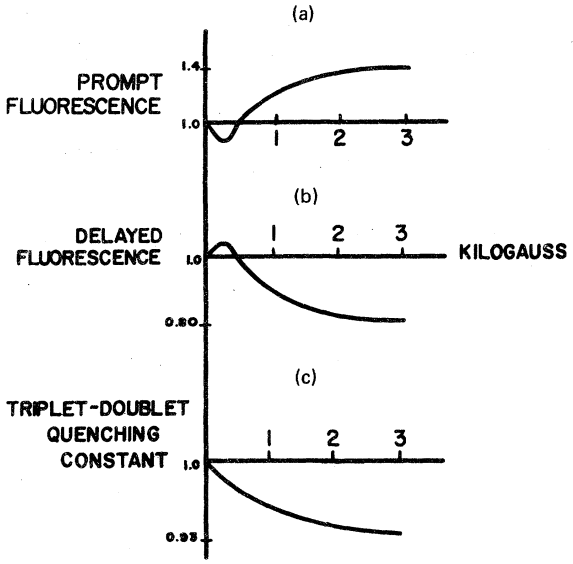

FIG. 2. Magnetic field dependence of some excitonic processes. (a) Prompt fluorescence of tetracene at room temperature (excited with uv or blue light, $S_1 \leftarrow S_0$ absorption) this magnetic field dependence is due to the fission process (Refs. 26 and 54). (b) delayed fluorescence of tetracene at low temperature excited with red light (Ref. 22) ($T_1 \leftarrow S_0$ absorption). The magnetic field dependence is due to the fusion process. (c) Triplet-doublet interaction. The interaction rate constant is decreased by the magnetic field (Ref. 33) as shown.

2(b). The magnitude of $\gamma_{rad} \approx 10^{-9}$ cm^3 sec^{-1}. This value is probably correct to within a factor of 2.[21,22,30] It is noteworthy that the value of γ_{rad} is about 200 times smaller in anthracene[13] than in tetracene.

C. Annihilation of singlet excitons by triplet excitons

In this process singlet excitons are quenched by a long-range (~ 50 Å) Förster-type-resonance energy transfer mechanism[31] in which T_1 is promoted to a higher triplet level T_2 or T_3, while S_1 decays to S_0. A singlet exciton is removed, but the triplet exciton remains according to the scheme

$$S_1 + T_1 \xrightarrow{\gamma_{st}} S_0 + T_1 \ . \tag{3}$$

It is predicted theoretically that γ_{st} is not magnetic field sensitive; it has a magnitude[30] of $\gamma_{st} \approx 2\times10^{-7}$ cm^3 sec^{-1}. In anthracene the value of γ_{st} is considerably smaller, i.e., γ_{st} (anthracene) $= (5\pm3)\times10^{-9}$ cm^3 sec^{-1} (see for example Fourny *et al.*[32] and the references cited therein).

D. Mutual annihilation of singlet excitons

An interaction of two singlet excitons results in the annihilation of one of these singlets:

$$S_1 + S_1 \xrightarrow{\gamma_{ss}} S_0 + S_1 \ . \tag{4}$$

The value for γ_{ss} in solid tetracene is not available, but in anthracene[16] it is $(1\pm0.5)\times10^{-8}$ cm^3 sec^{-1}. Since all the rate constants measured appear to be higher in tetracene than in anthracene, it is likely that γ_{ss} in tetracene lies between ~ 10^{-7}–10^{-8} cm^3 sec^{-1}.

E. Annihilation of excitons by doublet quenchers

Free holes or electrons (n_f^+, n_f^-), or trapped holes or electrons (n_t^+, n_t^-), or free radicals (n_r) are spin-$\frac{1}{2}$ particles and are known to quench both singlet and triplet excitons. In the case of triplet excitons,

$$T_1 + n \xrightarrow{\gamma_t} S_0 + n \ . \tag{5}$$

The n_f^+, n_f^-, n_t^+, n_t^-, or n_r are collectively denoted by n in Eq. (5). The quenching constant γ_t is known to be magnetic field sensitive[33–35] if n is paramagnetic and decreases monotonically with increasing field strength until saturation is reached at ~ 2500 G[33,34] [Fig. 2(c)].

The quenching-rate constant of triplets by trapped holes γ_{th} has been measured and its value is $\gamma_{th} = (5\pm2)\times10^{-9}$ cm^3 sec^{-1}. In anthracene this rate constant is smaller[36,37] and is equal to ~ 10^{-11} cm^3 sec^{-1}; the rate constant for quenching of triplets by trapped electrons γ_{te} in anthracene has the same value.

The rate constant for the quenching of triplet excitons by free electrons (γ_{te}^*) or by free holes (γ_{he}^*) has not yet been determined in tetracene. However, in anthracene, Wakayama and Williams[38] have found that $\gamma_{th}^* = 1.1\times10^{-9}$ cm^3 sec^{-1} and $\gamma_{te}^* = 6\times10^{-10}$ cm^3 sec^{-1}, whereas Frankevich *et al.*[39] obtained a smaller value of $\gamma_{th}^* = (2\pm1)\times10^{-10}$ cm^3 sec^{-1}.

The interactions in triplet-triplet fusion [Eq. (2)] and triplet-trapped carrier processes [Eq. (5)] are essentially nearest-neighbor interactions which depend primarily on the rate of formation of pair states, which in turn depends basically on the diffusion coefficient of triplet excitons. Therefore, the values of γ_{th}, γ_{te} and γ_{rad} are similar in anthracene. On the other hand the thermal velocities of free carriers are higher than that of triplet excitons and thus γ_{te}^*, $\gamma_{th}^* \gg \gamma_{th}$, γ_{te}.

The quenching of singlet excitons can proceed in two ways:

$$S_1 + n \xrightarrow{\gamma_{sn}} S_0 + n \ , \tag{6a}$$

$$S_1 + n \xrightarrow{\gamma'_{sn}} T_1 + n \ . \tag{6b}$$

A magnetic field dependence might be observable in Eq. (6b) but not in Eq. (6a). The exact mechanism of quenching of singlets has not been established; we shall therefore not make any distinctions between γ'_{sn} and γ_{sn} below. However, in anthracene[40] the rate constant for the quenching

of singlet excitons by trapped holes (γ_{sh}) or by trapped electrons (γ_{se}) is $\sim 10^{-8}$ cm^3 sec^{-1}, whereas in tetracene[40,41] this value is $\sim 10^{-7}$ cm^3 sec^{-1}.

F. Electron-hole recombination

Following the excitation of a neutral high-lying state of molecular excitation, an autoionization process occurs with relatively high efficiency resulting in the production of a free electron and hole. It is possible for this pair of carriers to recombine before they can interact with any other free charges which may be present in their immediate environment. Such recombination is kinetically first order and is referred to as geminate recombination. The time scale of this geminate recombination is so short ($\sim 10^{-11}$ sec) that the spin states of the correlated electron and hole pair do not relax; under these conditions, the recombination produces mostly singlet states, as was the case before ionization took place. In anthracene and tetracene the lowest excited singlet state which is thus produced has an energy lower than that of the band gap.[16]

If the electrons and holes produced by autoionization recombine with other carriers in a random fashion, the process is kinetically second order and the spins of the combining charges are uncorrelated. Under these conditions, the final states can be either a singlet or a triplet, and this recombination may be written

$$n^+ + n^- \xrightarrow{\gamma_{eh}} S_1 \text{ or } T_1 , \tag{7}$$

where n^+ and n^- denote the free holes and electrons, respectively. In anthracene[42] $\gamma_{eh} \sim 10^{-6}$ cm^3 sec^{-1}, while no measurement is available for tetracene. However, the value of γ_{eh} is not expected to be much different in tetracene since this constant depends on the electron and hole mobilities and on the dielectric constant, which are similar in these two crystals.

G. Temperature dependence of magnetic field effects in tetracene

It has been demonstrated that fission and fusion are reversible processes:

$$S_0 + S_1 + \Delta E \rightleftarrows T_1 + T_1 . \tag{8}$$

If the triplets that appear in Eq. (8) are excited directly ($T_1 \rightarrow S_0$) using red light, only a small magnetic effect $\sim(-1$ to $-2)\%$ on the fluorescence is observed at room temperature because of the opposing effects of the magnetic field on the forward and reverse reactions shown in Eq. (8). At low temperature, however, fission is suppressed and a negative effect on the delayed fluorescence of $\sim -30\%$ appears. The magnetic field dependence of this effect is shown in Fig. 2(b). Fission on the other hand, gives rise to a $\sim(20$–$40)\%$ increase in the prompt (uv-excited) fluorescence in the presence of a saturating magnetic field at room temperature, and no effect below 160 °K. Under experimental conditions where fission and fusion are operative simultaneously, as is the case in α-particle-bombarded tetracene crystals, the presence of either component can be revealed separately by varying the temperature, as will be shown below.

The rate constants of the different excitonic processes for tetracene and anthracene are compared and summarized in Table I and their magnetic field dependence, if any, is also indicated.

II. EXCITON PROCESSES IN α-PARTICLE TRACKS

An analysis of energy degradation processes in α-particle tracks in anthracene in terms of known excitonic phenomena has been made by Schott.[12] In this section some of the time scales of various quenching phenomena in crystalline tetracene are estimated and compared to those in anthracene.

We begin with some of the considerations outlined by Voltz.[11] The passage of a heavy ion through an organic medium results in the formation of plasmons and secondary (δ) electrons. The maximum energy of the secondary electrons is $T_{max} \cong 4mE/M$, where m is the mass of an electron, E is the energy and M is the mass of the primary particle. In our experiments $E \approx 4.4$ MeV and $T_{max} \approx 2.4$ keV.

In anthracene crystals the penetration depth of a 5.3-MeV α particle is 35 ± 1 μm.[43] For a 4.4-MeV α particle, using the range-energy relationships given in Ref. 1, the range is estimated to be between 25 and 30 μm in tetracene. This corresponds to an average energy deposition of ~ 1.4–1.8×10^9 eV/cm or ~ 10–20 eV/Å.

Voltz *et al.*[4] have given a theoretical expression for estimating the quantity F_s which gives the ratio of the energy lost by the primary particle in producing secondary electrons to the total energy loss:

$$F_s = \frac{1}{2} \frac{\ln(4mE/MT_0)}{\ln(4mE/MI)} , \tag{9}$$

where T_0 is the minimum energy of a secondary electron which allows it to escape out of the primary-particle track. For a track radius of ~ 150 Å, $T_0 \approx 500$ eV.[12] I is the mean excitation potential and is ~ 62 eV.[4] Using these values and Eq. (9) we obtain $F_s \approx 20\%$. Thus, most of the energy is deposited in the track of the primary particle. Furthermore, since the maximum energy of the secondary electrons is only ~ 2400 eV, the rate of energy loss of the secondaries will also be very high and thus ionization quenching will also prevail strongly in those regions of the crystal in which the secondary electrons lose their energy.

TABLE I. Rate constants for exciton interactions in crystalline anthracene and tetracene.[a]

Process	Tetracene	Anthracene	Magnetic field dependent
(1). Fission: $S_0+S_1 \xrightarrow{\gamma_f} T_1+T_1$	$\gamma_f \approx 1.5\times10^{-12}$ cm^3 sec^{-1}	negligible	Yes
(2). Fusion: $T_1+T_1 \xrightarrow{\gamma_{rad}} S_1+S_0$	$\gamma_{rad} \approx 10^{-9}$ cm^3 sec^{-1}	$\gamma_{rad} \approx 10^{-11}$ cm^3 sec^{-1}	Yes
(3). Singlet-triplet annihilation:			
$S_1+T_1 \xrightarrow{\gamma_{st}} S_0+T_1$	$\gamma_{st} \approx 2\times10^{-7}$ cm^3 sec^{-1}	$\gamma_{st} \approx 10^{-8}$ cm^3 sec^{-1}	No
(4). Singlet-singlet annihilation:			
$S_1+S_1 \xrightarrow{\gamma_{ss}} S_1+S_0$	...	$\gamma_{ss}=10^{-8}$ cm^3 sec^{-1}	No
(5). Annihilation of S_1 by free carriers:			
$S_1+n_f^{\pm} \xrightarrow{\gamma^*_{se(h)}} S_0+n_f^{\pm}$	...	$\gamma^*_{sh},\gamma^*_{se} \approx 10^{-8}$ cm^3 sec^{-1}	No
(6). Annihilation of S_1 by trapped carriers:			
$S_1+n_t^{\pm} \xrightarrow{\gamma_{se(h)}} S_0+n_f^{\pm}$	...	$\gamma_{sh},\gamma_{se} \approx 10^{-8}$ cm^3 sec^{-1}	?
(7). Annihilation of triplets by free carriers:			
$T_1+n_f^{\pm} \xrightarrow{\gamma^*_{te(h)}} S_0+n_f^{\pm}$	...	$\gamma^*_{th},\gamma^*_{te} \approx 10^{-9}$ cm^3 sec^{-1}	Yes
(8). Annihilation of triplets by trapped carriers:			
$T_1+n_t^{\pm} \xrightarrow{\gamma_{te(h)}} S_0+n_f^{\pm}$	$\gamma_{th}=(5\pm1)\times10^{-9}$ cm^3 sec^{-1}	$\gamma_{te},\gamma_{th} \approx 10^{-11}$ cm^3 sec^{-1}	Yes
(9). Singlet lifetime (no quenchers)	$\tau_s \approx 2\times10^{-10}$ sec (at 298 °K)	$\tau_s \approx 2\times10^{-8}$ sec	Yes (tetracene) No (anthracene)
(10). Triplet lifetime (no quenchers)	$\tau_T=(50-200)\times10^{-6}$ sec	$\tau_T > 20\times10^{-3}$ sec	No

[a]The rate constants are taken from the literature and in most cases have been rounded off: the references are given in the text (Sec. II).

For these reasons, the relative number of scintillations being produced by secondaries is not likely to exceed ~20%, and even this fraction of photons emanates from regions in which ionization quenching is similar, though not as effective,[12] as in the track of the primary particle. Because of the approximate nature of the calculations contained herein, the effect of the secondaries can be neglected, at least for the α-particle energies used in this work.

With these considerations, the lower limit of energy deposition in the α-particle track is estimated to be ~10 eV/Å. The g value for the production of plasmons in aromatic media is taken to be ~4–5,[11] and it is assumed that each plasmon decays within ~10^{-15} sec to a superexcited state. A superexcited state in an organic crystal can be viewed as a highly excited electronic and vibronic exciton state of relatively large spatial extent which may decay by a radiationless process to a lower exciton state, by autoionization into an electron-hole pair, or by a chemical dissociation leading to a chemically transformed molecule or radical pair in the lattice.

Using a track radius of $R_0 \approx 150$ Å, the density of superexcited states which are formed in the early stages of radiation are estimated to be ~10^{19} excitations cm^{-3}. The dominant decay mechanism of superexcited states appears to be the formation of singlet excitons and autoionization into an electron-hole pair within about ~10^{-13}–10^{-14} sec. Triplets are not formed effectively by the decay of superexcited states because of spin-selection rules. Autoionization may be the dominant mode of decay since the autoionization efficiency in the gas phase is ~0.8.[44–46] In condensed media such as organic crystals a similar yield of electron and holes may be expected. Perkins[47] has estimated that 27–30 eV are required to form one initial electron-hole pair, while $\gtrsim$400 eV are required per pair of actually collected carriers in x-ray-bombarded anthracene. This indicates that recombination limits the number of carriers collected and that the autoionization efficiency of superexcited states in anthracene is in the range of 0.7–0.9 (depending on the value of either 20–25 eV which is assigned to the superexcited state). This result is consistent with the autoionization efficiency estimated from gas-phase studies. The difference between the solid state and the gas phase lies in the fact that in the crystal, rapid geminate and random recombination of electrons and holes can take place. This process is the most important source of triplet excitons which also gives

rise to the continuing production of singlet excitons long after the passage of the α particle.

The g value for the production of singlet excitons in anthracene can be deduced from studies on anthracene excited by fast electrons under conditions when ionization quenching is minimal. About 50–60 eV are deposited in anthracene per singlet exciton produced under these conditions.[1] A g value of 1.6–2.0 is obtained which gives an upper limit of ~0.3–0.5 for the quantum yield of singlets from the decay of superexcited states or plasmons.

The formation of chemically transformed molecules (permanent quenchers) is by far the most important long-term effect of the passage of heavy ions, but the g value is much lower than that for the production of excitons and carriers and is thus neglected in these rough calculations. (The g value is estimated to be ≈ 0.1 from the data of Northrup and Simpson,[48] who estimated 70 Å as the distance between permanent quenching centers produced along an α-particle track.)

For purposes of a rough calculation we assume that the efficiency of production of singlets from superexcited states is ~0.3 and that of electron-hole pairs is ~0.7. Based on an initial plasmon concentration of about 10^{19} cm^{-3}, one estimates that the initial densities of singlets and electron-hole pairs are

$$[S_1] \sim 3\times 10^{18} \text{ cm}^{-3},$$
$$[n^*] \approx 7\times 10^{18} \text{ cm}^{-3}.$$

These densities are enormous and correspond to an excitation of approximately one out of 500 molecules in the track (there are a total of ~3×10^{21} molecules cm^{-3}). This gives an average distance of 30–40 Å between adjacent electrons, holes, and singlet excitons.

A. Evolution of excited states

The events described above occur on a time scale of 10^{-14} sec of less. The excited states which are formed by these primary energy-degradation processes evolve over a much longer time period.

Initially, we assumed that only singlet excitons and electron-hole pairs are created as described in the previous section. The likely events that follow the initial excitation are: (i) diffusion of singlet excitons and carriers out of the track, (ii) electron-hole recombination with the accompanying formation of triplet excitons and additional singlet excitons, (iii) singlet-singlet annihilation giving rise to the disappearance of one singlet per annihilation event, (iv) quenching of singlet excitons by charge carriers and by triplet excitons, and (v) triplet-triplet exciton fusion and triplet-doublet quenching.

The time scales of these processes can be estimated if it is assumed that the rate constants measured under conditions of weak excitation (photoexcitation) are not radically different in regions of high densities of excitation. While this has not been established, our calculations are only approximate in any case, so that this approximation is not a severe restriction unless the rate constants are different by more than a factor of 10.

B. Diffusion out of the track

For cylindrical symmetry a characteristic diffusion time t_d can be specified which is

$$t_d \approx R_0^2/4D; \tag{10}$$

R_0 is the track radius, D is the diffusion coefficient, and t_d is equal to the time required to reduce the density of excited species at the center of the track by a factor of 2.

The largest diffusion coefficient for either the holes or singlet excitons in tetracene is estimated to be at most 10^{-2} cm^2 sec^{-1}. Using a track radius of 150 Å yields a diffusion time of $t_d \approx 5\times 10^{-11}$ sec. Thus, excitation densities of even highly mobile singlet excitons or carriers are not likely to change significantly as a result of diffusion on time scales less than ~5×10^{-11} sec.

C. Carrier recombination

Because of the extremely high carrier densities in tracks of ionizing particles, random recombination of electron-hole pairs can occur. Schott[12] concludes that random recombination dominates over geminate recombination in such cases. Both singlet and triplet excitons can then be formed. On a time scale of $< 10^{-8}$ sec the ratio of triplets to singlets formed will be 3:1, since normal spin statistics apply to random recombination. On the time scale $> 10^{-8}$ sec, intersystem crossing $S_1 \rightarrow T_1$ may be important and the ratio of triplets to singlets formed may therefore be larger. However, quenching processes within the track will be much more probable than intersystem crossing, which can thus be neglected here.

Carriers must move an average distance of 20–25 Å before recombination can occur. With velocities of the order of ~10^6 cm/sec, this requires a minimum time of ~$(2–3)\times 10^{-13}$ sec. Because of this, the extent of recombination on time scales much less than a picosecond is thus probably very small. In any case such short time domains are experimentally inaccessible and will be designated here as time domain I.

The time interval in which carriers can recombine to form triplet and singlet excitons, but remain essentially within the track radius is designated as time domain II. It is characterized by a time interval t_{II} which is approximately given by

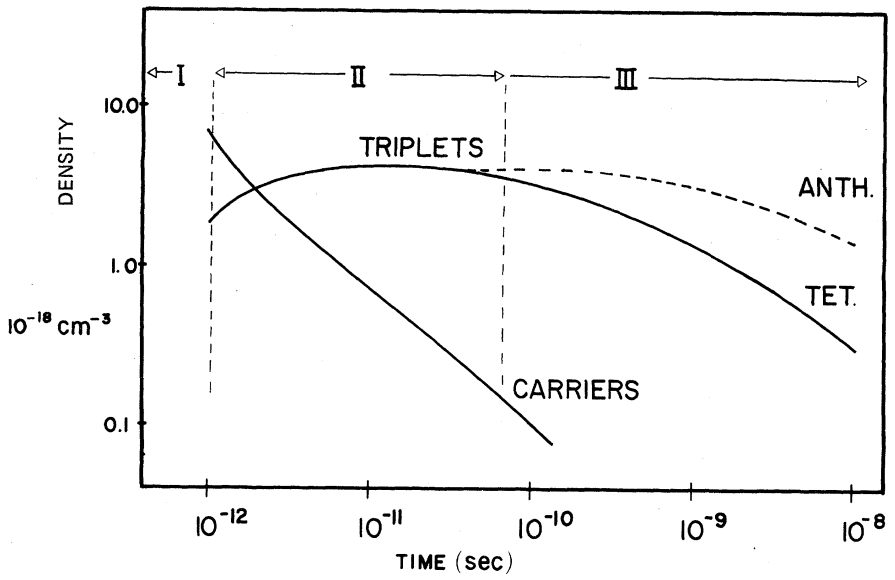

FIG. 3. Estimated carrier and triplet exciton densities in an α-particle (~4.4 MeV) track. Time domain I: $<10^{-12}$ sec, recombination of carriers is relatively unimportant. Time domain II: 10^{-12} sec $< t < t_d$, where t_d is the approximate characteristic diffusion time of excitons out of the track. Note that t_d is longer in anthracene than in tetracene. Time domain III: $t > t_d$.

$$10^{-12} < t_{II} < t_d \text{ sec} .$$

The time domain III is specified by $t_{III} > t_d$.

In the final stage of the process of thermalized electron-hole recombination, a charge-transfer (CT) exciton state is presumably formed prior to the appearance of the singlet or triplet excited state. If the lifetime of the CT exciton is longer than 10^{-11} sec (lifetimes of the order of 10^{-9} sec have been proposed[49]) then obviously, one cannot propose that the usual Frenkel-type singlet and triplet excitons are created by carrier recombination in times shorter than the CT exciton lifetime. On the other hand, if singlet and triplet excitons are actually produced by thermalized carrier recombination in times $\lesssim 10^{-11}$ sec, then the CT exciton formed from the thermalized electron-hole recombination has a lifetime $\lesssim 10^{-11}$ sec. CT excitons may behave in some respects like Frenkel singlet or triplet excitons and in the absence of more concrete data, it will be assumed herein that singlet and triplet excitons are formed in short times.

In time domain II, the density of carriers is approximately described by a simple second-order equation, since the effects of diffusion out of the track are negligible:

$$\frac{1}{n_f^{\pm}(t)} = \frac{1}{n_f^{\pm}(0)} + \gamma_{eh} t \, , \tag{11}$$

where $n_f^{\pm}(0)$ is the initial carrier density at $t \approx 10^{-12}$ sec [which is taken as $t = 0$ in Eq. (11)]. The carrier density as a function of time estimated according to Eq. (11) is shown in Fig. 3. In this calculation, the effect of geminate recombination is neglected for simplicity.

D. Characteristic exciton-annihilation time scales

Within time domain II, excitons are subject to various annihilative processes and the characteristic decay times as a function of particle density can be estimated from the relations

$$\gamma_{ss}[S_1] = \text{rate of quenching of } S_1 \text{ via } S_1\text{-}S_1 \text{ annihilation}, \tag{12}$$

$$\gamma_{st}[T_1] = \text{rate of quenching of } S_1 \text{ via annihilation by } T_1, \tag{13}$$

$$\gamma^*_{se(h)}[n_f^{\pm}] = \text{rate of quenching of } S_1 \text{ by free carriers}, \tag{14}$$

$$\gamma^*_{te(h)}[n_f^{\pm}] = \text{rate of quenching of } T_1 \text{ by free carriers}, \tag{15}$$

$$\gamma_{rad}[T_1] = \text{rate of annihilation of triplets by fusion (= rate of appearance of } S_1 \text{ via fusion channel)}. \tag{16}$$

In Eqs. (12)–(16) the bracketed quantities refer to the number of singlet excitons, triplet excitons, or free carriers per cm^3.

The various rate constants are summarized for convenience in Table I for both anthracene and tetracene. We note that in the case of anthracene

γ_{rad}, γ_{te}, and γ_{th} have approximately the same value. In tetracene γ_{th} appears to be a little larger than γ_{rad}, but it is likely that this difference is due to experimental uncertainties. In anthracene, $\gamma_{st} \approx \gamma_{ss} \approx \gamma^*_{se(h)} \approx \gamma_{se(h)}$ because all of these processes are determined by the diffusion coefficient of the singlet exciton. Thus, while some of these rate constants have not been measured in tetracene, it is reasonable to assume that in this crystal the rate constants γ_{ss}, etc. will also be similar in value to γ_{st}.

The scintillation efficiency in organic crystals bombarded by α particles will depend on the magnitude of the quenching rates [(12)–(15)] relative to the intrinsic decay constant τ_s^{-1} of the singlet excitons.

The quenching rates as a function of particle densities are plotted in Fig. 4 and compared to τ_s^{-1} for both anthracene and tetracene. The quenching rate $\gamma_{st}[T_1]$ is plotted as a function of the triplet exciton density $[T_1]$. Since we are interested at this point in the order of magnitudes of the various processes rather than exact calculations we can assume that $\gamma_{st} \approx \gamma^*_{se(h)} \approx \gamma_{ss}$, and that $\gamma_{st}[T_1] \approx \gamma_{ss}[S_1] \approx \gamma^*_{se(h)}[n_f^{\pm}] \approx \gamma_{se(h)}[n_t^{\pm}]$ if $[T_1] \approx [S_1] \approx [n_f^{\pm}] = [n_t^{\pm}]$. Similarly, since $\gamma_{rad} \approx \gamma_{te(h)}$, the $\gamma_{te(h)}[n_t^{\pm}]$ curve is approximately the same as the $\gamma_{rad}[T_1]$ curve if $[T_1]$ is replaced by $[n_t^{\pm}]$ in Fig. 4. All of these quenching rates can then be estimated from the plots shown in Fig. 4.

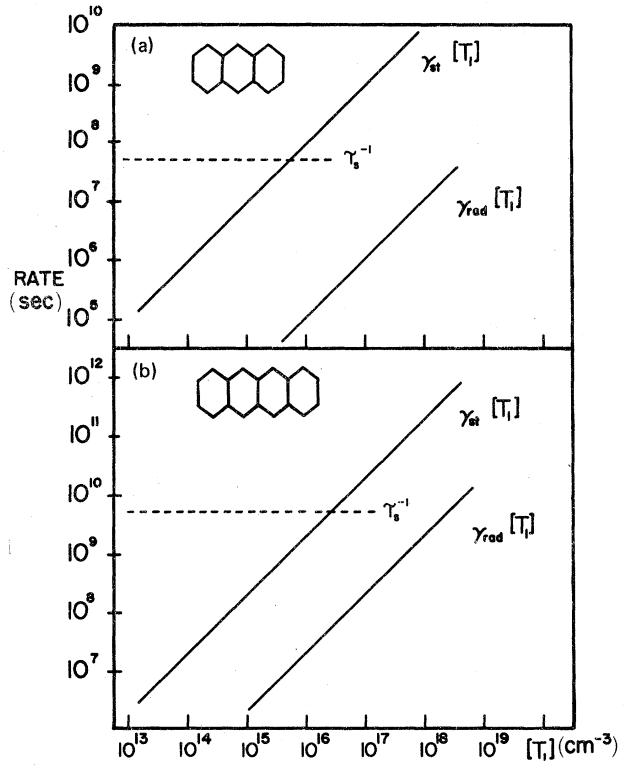

FIG. 4. Estimated rate of annihilation of singlet excitons by triplets ($\gamma_{st}[T_1]$) and of triplet excitons by fusion ($\gamma_{rad}[T_1]$) as a function of triplet-exciton density $[T_1]$. (a) Anthracene, fluorescence decay time of singlets is $\tau_s \approx 2\times10^{-8}$ sec in the absence of quenching. (b) Tetracene, $\tau_s \approx 2\times10^{-10}$ sec. The quenching rates of excitons by carriers can also be estimated from these plots because of the similarities in the rate constants (see text).

The triplet density within the track is depleted by fusion, quenching, and diffusion. The fastest quenching process is the interaction of triplets with free carriers and this rate is characterized by $\gamma^*_{te(h)}[n_f^{\pm}]$. The free-carrier density diminishes rapidly with increasing time within time domain II. Using an estimated value of $\gamma_{te(h)} \sim 10^{-7}$ cm^3 sec^{-1}, we obtain $(\gamma^*_{te(h)}[n_f^{\pm}])^{-1} \gtrsim 10^{-10}$ sec at $t \sim 10^{-11}$ sec, when the carrier density is $\sim 10^{17}$ cm^{-3} (Fig. 3). This represents the lowest limit for the triplet lifetime at $t \sim 10^{-11}$ sec. The importance of this quenching channel should now be compared to the decrease in the triplet-exciton density brought about by diffusion of triplets out of the track. The characteristic diffusion time t_d is the factor which defines the onset of time domain III. Since in tetracene all of the rate constants involving triplets appear to be at least 100 times faster than in anthracene, we estimate that the diffusion constant D_T for triplets is at least 10–50 times larger in tetracene than in anthracene. In anthracene D_T in the ab plane[50] is $\sim 10^{-4}$ cm^2 sec^{-1}. In tetracene therefore $D_T \sim 10^{-2}$–10^{-3} cm^2 sec^{-1}, which yields a t_d value in the range of 5×10^{-11}–10^{-10} sec in tetracene. This time is shorter or comparable to the quenching time $(\gamma^*_{te(h)}[n_f^{\pm}])^{-1}$ and its effect in calculating the triplet-exciton density for $t > 10^{-11}$ sec will be neglected for simplicity. Thus, within time domain II, there will be an interval in which the triplet-exciton density remains approximately constant. Utilizing the assumptions that triplet excitons are formed by the recombination of free carriers, that the quenching of singlets by triplets does not deplete the $[T_1]$ density, and that the triplet-exciton quenching mechanisms are inefficient on time scales $t < 10^{-10}$ sec, $[T_1]$ is given by Eq. (17) (as long as $t \ll t_d$):

$$T_1(t) \approx \tfrac{3}{4} n_f^{\pm}(0)\left(1 - \frac{1}{1+\gamma n_f^{\pm}(t)}\right). \qquad (17)$$

Using the $n_f^{\pm}(0)$ value of $\sim 7\times10^{18}$ for the initial carrier density, a plot of Eqs. (17) and (11) is given in Fig. 3 which shows the plateau in $T_1(t)$ within time domain II.

Since in this time domain the triplet-exciton density is higher than the free-carrier density, the lifetime of the singlet excitons appears to be limited by the most efficient quenching channels, which are the singlet-singlet and singlet-triplet channels. The singlet-singlet channel re-

one singlet exciton per event and the quenching rate diminishes with each singlet removal, while in the case of the singlet-triplet channel, one singlet exciton disappears while the triplet-exciton density (and hence the singlet-exciton quenching rate) remains constant. Therefore, with increasing time in domain II, the most important quenching channel for singlets is their annihilation by triplet excitons.

The effectiveness of this quenching channel relative to the intrinsic singlet-exciton lifetime is indicated in Fig. 4. For tetracene, the singlet lifetime is dominated by triplet-exciton quenching as long as $[T_1] \gtrsim 5\times10^{16}$ cm^{-3}, while in anthracene this quenching channel dominates as long as $[T_1] \gtrsim 5\times10^{15}$ cm^{-3}.

These limiting densities depend on the accuracy of the experimentally determined γ_{st} quenching constant. According to Ern *et al.*[30] there is an uncertainty within a factor of 10 for γ_{st} in tetracene; however, we note that the largest bimolecular rate constant is that for electron-hole recombination in these organic crystals which is $\gamma_{eh} \sim 10^{-6}$ cm^3 sec^{-1}. Thus, γ_{st} is probably equal to or smaller than 2×10^{-7} cm^3 sec^{-1} (but not larger), while it is greater than 10^{-8} cm^3 sec^{-1}, which is the corresponding value in anthracene. Thus, the lifetime-limiting triplet-exciton density in tetracene could be a factor of ten larger than calculated above.

We note from the $\gamma_{rad}[T_1]$ curve in Fig. 4 that the contribution of the fusion term to the $[S_1]$ population will be negligible in time domain II and is important only on longer time scales within time domain III.

The triplet density will remain fairly constant for longer times ($\sim 10^{-9}$ sec) in anthracene than in tetracene (5×10^{-11}–10^{-10} sec). In agreement with Schott,[12] we postulate that this "sea" of triplet excitons in time domain II for both crystals constitutes the most probable source of quenching of singlets. These triplet excitons (and the free carriers) are therefore identified as the *transient* quenching centers defined by Birks.[1] Free carriers also contribute to the quenching of singlets; their effect is most important only in the early time intervals of domain II and decreases as the density of free carriers diminishes.

The diffusion out of the track is 50–100 times faster in tetracene than in anthracene which shortens the time domain II considerably and thus reduces the extent of quenching. Thus, even at low temperatures (< 160 °K) where fission is suppressed and the S_1-decay time is similar in anthracene and tetracene, the effects of *transient* quenchers, i.e., triplet excitons, may be less severe in tetracene than in anthracene.

To summarize this section, the major conclusion of some simple considerations are

(a) Singlet excitons are initially formed by decay of superexcited states and later by electron-hole recombination. For convenience we shall refer to these singlets as primary singlet excitons, in contrast to the secondary singlets formed *indirectly* by fusion. Directly formed S_1 states contribute to the prompt scintillation component L_P and the indirectly formed singlets to the delayed component L_D. These are distinguishable by magnetic field effects which give rise, in tetracene, to the field dependence shown in Fig. 2(a) (L_P) and Fig. 2(b) (L_D).

(b) Random or columnar recombination[12] gives rise mostly to triplet excitons.

(c) The directly formed singlets are quenched by other singlets, by free carriers, and by triplet excitons. These processes are more efficient in anthracene than in tetracene, since in the latter case fission can compete with quenching on the time scale of 2×10^{-10} sec and the singlet-exciton lifetime is already quite short at room temperature. At low temperatures, tetracene and anthracene should be nearly alike in their response to α particles. However quenching phenomena within the track are predicted to be more effective in anthracene because of the lower rate of diffusion of excitons out of the track.

The different modes of generation of singlet excitons and the quenching of excitons in α-particle tracks are summarized in Fig. 5.

The major assumptions which were made in arriving at the conclusions in this section of the paper are as follows:

(1) The track radius $R_0 \simeq 150$ Å is probably correct to within a factor of 2 and any errors in this value would affect the characteristic diffusion time t_d, the calculated characteristic quenching rates, and the exciton densities. All calculated quantities, however, would be scaled in the same direction.

(2) The g value (yield per 100 eV deposited) for the formation of excitons or ionized states is of the order of 4–5. The evidence indicating that these values are in the correct range has been discussed by Voltz.[11]

(3) The initial formation of ionized states is ~70% efficient. An error in this value would not be too crucial either, since it would only affect the absolute number of triplets formed. Based on the g value for the formation of carriers in organic media,[11] the ionization efficiency used here appears to be reasonable.

(4) The dynamic rate constants used here were determined under conditions of relatively low exciton and carrier densities using photoexcitation. Whether these rate constants apply at the short time scales discussed here and at the high carrier and exciton densities which prevail in the

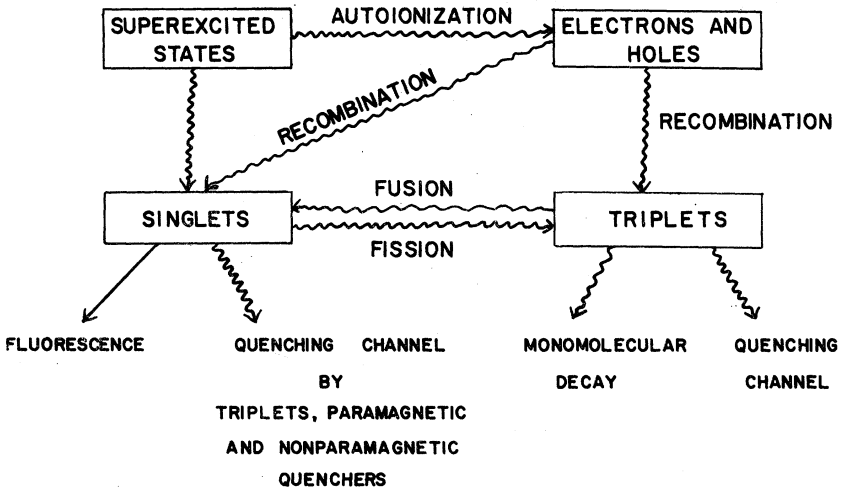

FIG. 5. Summary of processes in an α-particle track which can account for the generation and disappearance of excitons (diffusion is omitted for simplicity in the diagram).

α-particle tracks remains to be elucidated.

(5) In calculating the average amount of energy deposited per unit length of the tracks, the Bragg-curve effect was neglected. The Bragg curve describes the amount of energy deposited per unit track length; this increases as the penetration depth of the α particle increases and reaches a maximum at the end of the track.

Unless there are very drastic differences in the rate constants, or the value of the track radius R_0, the picture evolved here and elsewhere[12] for the dynamic processes in α-particle tracks appears to be reasonable. It is based on the current state of knowledge of exciton dynamics in organic crystals.

Fortunately, the magnetic field effects provide some insight into the mechanism of scintillation and the quenching processes which have an effect on the scintillation, and thus can be utilized to check some of the predictions discussed above.

III. BASIC KINETIC EQUATIONS FOR SCINTILLATION

Because of the low dosages in our experiments we need only consider the kinetics of the excitations within a given α-particle track. Furthermore, as discussed in Sec. II of this paper, the total scintillation L originating from a given track consists of a prompt component L_P which arises from singlet excitons which were either directly formed by internal conversion from the superexcited state or by electron-hole recombination, and a delayed component L_D resulting from the bimolecular reaction between two triplet excitons. The kinetics of the prompt and the delayed scintillation component were described initially by Voltz and Laustriat,[51,52] however, because of the exciton fission channel operative in crystalline tetracene their equations must be modified in a significant manner. We employ their notation where convenient.

A. Prompt component L_P

Let $C_S(\vec{r}, t)$ denote the primary singlet-exciton density at position $\vec{r}$ at time t within a given track. $C_S(\vec{r}, t)$ obeys the equation

$$\frac{\partial C_S(\vec{r}, t)}{\partial t} = D_S \nabla^2 C_S(\vec{r}, t) - \frac{1}{\tau_S} C_S(\vec{r}, t) , \qquad (18)$$

where D_S is the singlet diffusion coefficient and τ_S is the fluorescence decay time of the singlet excitons. We denote by $[Q_T]$ the density of *transient* quenchers and $[Q_P]$ the number of induced *permanent* quenchers in time domain II. The total-quencher density in this time domain is $[Q]=[Q_T]+[Q_P]$. These permanent quenchers can either be paramagnetic or nonparamagnetic in nature; the distinction will be made where necessary. The singlet-exciton lifetime (*primary singlets only*) is

$$\tau_S = \frac{1}{k_f(T, \vec{H}) + \gamma([Q_T]+[Q_P]) + k_F} , \qquad (19)$$

where γ is the quenching rate constant which is taken to be independent of the type of quencher since it primarily depends on the diffusion rate of singlet excitons, $k_f(T, \vec{H})$ is the fission rate at field strength $\vec{H}$ and temperature T, and k_F represents the radiative-decay rate (we have neglected nonradiative rates such as intersystem crossing which are known to be small in tetracene[26]). To an excellent approximation, the diffusion of singlets can be neglected for the time scales involved ($\lesssim 10^{-10}$ sec), so that

$$L_P(\vec{H}, T) = \int_0^\infty I_P(t)\, dt = k_F N_P \tau_S(\vec{H}, T) , \qquad (20)$$

where $I_P(t)$ denotes the scintillation intensity at time t, and N_P the total number of primary sin-

glets per track.

B. Delayed component L_D

The delayed component of the scintillation L_D is determined from the local density of delayed or secondary singlets $C_S'(\vec{r}, t)$ which obeys the equation

$$\frac{\partial C_S'(\vec{r}, t)}{\partial t} = D_S \nabla^2 C_S'(\vec{r}, t) - \frac{C_S'(\vec{r}, t)}{\tau_S'(\vec{H}, T)} + \frac{\gamma_{rad}(\vec{H})}{2} C_T^2(\vec{r}, t), \tag{21}$$

where $C_T(\vec{r}, t)$ denotes the local concentration of triplet excitons within the track, $\gamma_{rad}(\vec{H})$ is the radiative-fusion constant, and τ_S' is the singlet (indirect) lifetime which because of the time scales involved (time domain III) is different from τ_S, the lifetime of the primary singlets. Thus,

$$\tau_S'(\vec{H}, T) = \frac{1}{k_f(\vec{H}, T) + k_F + \gamma([Q_P'] + [Q_T'])} \gtrsim \tau_S \ . \tag{22}$$

$[Q_P']$ as in Eq. (19) is the density of permanent quenchers, while $[Q_T']$ is the density of transient quenchers in time domain III. The density of transient quenchers should be smaller in time domain III than in II, thus $[Q_T'] < [Q_T]$. The local density of triplet excitons is governed by the equation

$$\frac{\partial C_T(\vec{r}, t)}{\partial t} = D_T \nabla^2 C_T(\vec{r}, t) - \frac{1}{\tau_T} C_T(\vec{r}, t) - \gamma_{tot}(\vec{H}) C_T^2 + 2k_f(\vec{H}) C_S'(\vec{r}, t); \tag{23}$$

D_T is the triplet-exciton-diffusion coefficient, γ_{tot} is the total-rate constant for the disappearance of triplets, and the last term represents the production of triplets by exciton fission as discussed in Sec. I of this paper. Solving Eqs. (22) and (23) simultaneously presents mathematical difficulties because of their nonlinear character. Without serious loss of accuracy we can neglect the diffusion of the singlet excitons and assume steady-state conditions because of the short singlet lifetime particularly at room temperature. Thus, Eq. (21) gives

$$C_S'(\vec{r}, t) \approx \tau_S'(\vec{H}, T)[\tfrac{1}{2}\gamma_{rad}(\vec{H})] C_T^2(\vec{r}, t) \ . \tag{24}$$

Defining

$$\gamma_{eff}(\vec{H}, T) = \gamma_{tot}(\vec{H}) - k_f(\vec{H}, T)\tau_S'(\vec{H}, T)\gamma_{rad}(\vec{H}), \tag{25}$$

which is always greater than zero, the equation for the time evolution of the triplet-exciton density within a given track becomes

$$\frac{\partial C_T(\vec{r}, t)}{\partial t} = D_T \nabla^2 C_T(\vec{r}, t) - \frac{1}{\tau_T} C_T(\vec{r}, t) - \gamma_{eff}(\vec{H}) C_T^2(\vec{r}, t) \ . \tag{26}$$

From Eq. (21), the delayed scintillation intensity at time t, $I_D(t)$ obeys the equation

$$\frac{dI_D(t)}{dt} + \frac{1}{\tau_S'} I_D(t) = f(t) = k_F \frac{\gamma_{rad}(\vec{H})}{2} \int_v C_T^2(\vec{r}, t)\, dv \ , \tag{27}$$

where the integration is over the entire volume of the track.

For the case where the initial triplet density has a Gaussian spatial distribution with the origin at the center of the track, Voltz and co-workers have solved Eq. (26). This track distribution is considered as a sufficiently accurate description for an α-particle track. The solution is

$$f(t) = \frac{k_F \gamma_{rad}(\vec{H})}{4t_b \gamma_{eff}(\vec{H}, T)} \frac{N_T(0)\, e^{-2t/\tau_T}}{(1 + (t_a/2t_b)\exp(t_a/\tau_T)\{\mathrm{Ei}[-(t+t_a)/\tau_T] - \mathrm{Ei}(-t_a/\tau_T)\})^2 (1 + t/t_a)} \ , \tag{28}$$

where

$$t_a = R_0^2/4D_T \text{ and } t_b = [\gamma_{eff}(\vec{H}, T)\, C_T(0)]^{-1};$$

$N_T(0)$ is the total number of initially created triplet excitons from electron-hole recombination and

$$C_T(0) = N_T(0)/l\pi R_0^2 \ , \tag{29}$$

where R_0 is the radius of the track and l is its length,

$$\mathrm{Ei}(x) = -\int_x^\infty \frac{e^{-\alpha}}{\alpha}\, d\alpha \ . \tag{30}$$

The delayed scintillation component at time t follows from Eq. (27)

$$I_D(t) = k_F \frac{\gamma_{rad}(\vec{H})}{2} \int_0^t e^{-(t-\tau)/\tau_S'} f(\alpha)\, d\alpha \tag{31}$$

and the total delayed scintillation L_D

$$L_D(\vec{H}, T) = k_F \frac{\gamma_{rad}(\vec{H})}{2} \int_0^\infty I_D(t)\, dt \ . \tag{32}$$

It is possible to give a simple form to $L_D(\vec{H}, T)$ in general, however when $t < \tau_T$ and $t > \tau_S'$ Eq. (32) reduces to

$$L_D(\vec{H}, T) = \frac{k_F \tau_S'(\vec{H}, T)\gamma_{rad}(\vec{H})}{2\gamma_{eff}(\vec{H}, T)} N_T(0) \ . \tag{33}$$

The measured scintillation in our experiments can be analyzed, at least under conditions of small dosages, by the equations

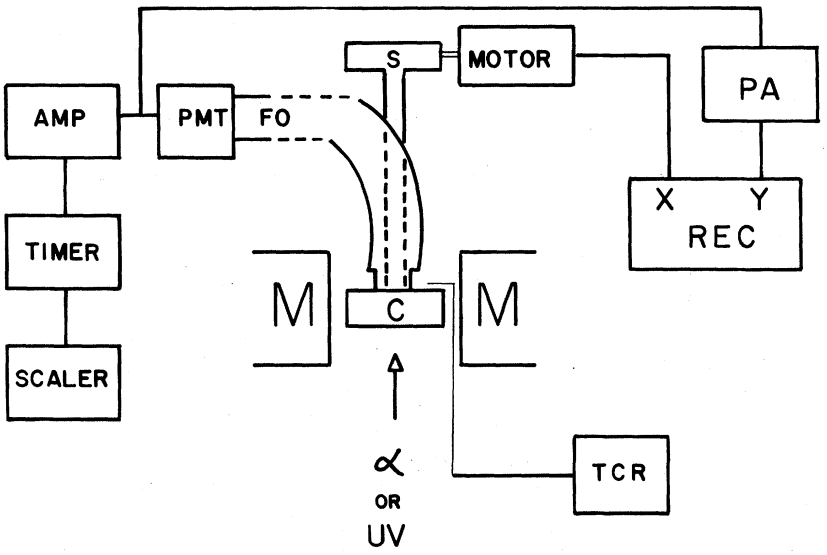

FIG. 6. Experimental arrangement, C—crystal, M—poles of magnet, FO—fiber optic, PMT—photomultiplier tube, AMP—preamplifier and amplifier, S—shaft attached to motor, PA—picoammeter, REC—recorder, TCR—thermocouple and recorder.

$$L(\vec{H},T)=L_P(\vec{H},T)+L_D(\vec{H},T)\ ,$$
$$L(\vec{H},T)=k_F N_P \tau_S(\vec{H},T)+\frac{k_F \tau_S'(\vec{H},T)\gamma_{rad}(\vec{H})}{2\gamma_{eff}(\vec{H},T)}N_T(0)\ . \quad (34)$$

IV. EXPERIMENTAL

A. Tetracene crystals

Tetracene powder was subjected to vapor-gradient-zone purification and single-crystal flakes approximately 10–40 μm in thickness were grown by sublimation in an atmosphere of argon.

B. Apparatus

The experimental arrangement is shown in Fig. 6. The crystals were mounted on a glass support which in turn was attached to a shaft extending out of the magnet. The crystals and the tip of the shaft to which the crystal was attached were placed in a light-tight chamber between the poles of the electromagnet. The shaft was fitted with a goniometer and attached to a slow ($\frac{1}{4}$ rpm) motor which could rotate the shaft and the crystal around an axis which was perpendicular to the direction of the magnetic field. This motor also drove the horizontal axis of an XY recorder. The magnetic field strength was regulated by means of a low-voltage power supply and was monitored with a gaussmeter. The scintillations were picked up by a 20-ft-long fiber optic which was fitted with a Corning 3-68 filter (in front of the fiber optic). The photomultiplier was an S-11 Bailey 4242B tube which was mounted inside a section of a heavy cast-iron pipe about ten feet away from the magnet to minimize stray magnetic field effects.

The output of the photomultiplier tube was fed into a preamplifier, amplifier, and a timer and then into a scaler. It was verified that only single-photon events were counted. The lower discriminator setting was adjusted to eliminate most of the low-voltage pulses. The pulse-height distribution was then determined and it was ascertained that there was only one maximum which had the same position and roughly similar width with the photomultiplier shutter either opened or closed. Furthermore, neither the position nor the width varied when the scintillation intensity was deliberately reduced by introducing neutral-density filters in the optical path. The count rate varied depending on the sample and was typically of the order of several thousand counts/sec and never exceeded 15 000 counts/sec (for anthracene). The pulses were counted as follows: with the magnetic field off, the counts were accumulated for 40 sec. The magnetic field was then adjusted to the desired value and the scintillations were counted for 80 sec. The field was then reduced to zero and scintillations were counted for another 40 sec period and this value was added to the previous 40-sec field-off value giving the total number of counts $L(0)$ in 80 sec with $\vec{H}=0$. This counting sequence tended to compensate for the slight deterioration of the scintillations as a function of time of exposure of the crystal to the α-particle source. The magnetic field effect was calculated according to the expression

$$\frac{\Delta L(\vec{H})}{L(0)}=\frac{L(\vec{H})-L(0)}{L(0)}\ .$$

The background counts for tetracene were at least ten times smaller than the scintillations and were subtracted from the total number of counts before calculating $\Delta L(\vec{H})/L(0)$.

C. Orientation of the crystal in the magnetic field

The magnitude of the magnetic field effect on the uv-excited photofluorescence F is a strong function of the orientation of $\vec{H}$ with respect to the crystallographic axes. For each 180° of rotation of the crystal with $\vec{H}$ lying in the *ab* plane of the tetracene crystals there are two sharp maxima in $\Delta F(\vec{H})/F(0)$ about 53° apart with the *b* crystallographic axis lying between these two peaks.[20] These maxima characterize the resonance directions in the given plane.

It was ascertained that α-particle scintillation $[\Delta L(\vec{H})/L(0)]$ exhibited similar though much smaller maxima at the same orientations as the maxima of $\Delta F(\vec{H})/F(0)$. This showed that the magnetic field effect on the scintillation is traceable to the same excitonic phenomena which occur in photoexcitation. In addition, further proof was obtained from the magnetic-field-strength dependence of $\Delta L(\vec{H})/L(0)$, which in all cases studied showed the behavior depicted in Fig. 2(a) or Fig. 2(b). All of the results reported here were obtained with the magnetic field lying in the *ab* planes of either the tetracene or anthracene crystals oriented along one of the resonance directions. The resonance directions were determined by replacing the α-particle source by a 100 W mercury-xenon arc lamp and monitoring the photofluorescence intensity as a function of the magnetic field orientation in the *ab* plane. A quartz light guide was utilized to illuminate the crystal inside the magnet and a Corning 7-37 filter (366 mm band pass) was interposed between the lamp and the light guide. With the arrangement shown in Fig. 6, there was a 20% stray-light component (80% crystal fluorescence) in the output of the photomultiplier which was connected to a picoammeter. This amount of stray light presented no problem in locating the resonance. The resonances were located by slowly rotating the crystal and looking for peaks in the photomultiplier output on the *XY* recorder.

D. Low-temperature studies

The temperature was varied by passing dry nitrogen through liquid nitrogen and blowing this cooled nitrogen onto the crystal. The temperature inside the light-tight chamber was monitored by means of a copper-constantan thermocouple placed next to the crystal.

E. α-particle source

The α-particle source was a 0.67-mCi 5.3-MeV 241 Am source. However, the energy of the α-particle impinging on the *ab* plane of the crystals was only ~4.4 MeV, because the surface of 241 Am was covered with a thin aluminum foil for safety reasons. The crystals were about 5 mm away from the surface of the source and the number of particles incident on the crystal was determined with a Geiger counter and found to be $\sim 2\times10^5$ particles $\text{sec}^{-1}\ \text{cm}^{-2}$.

V. MAGNETIC FIELD DEPENDENCE OF THE TOTAL SCINTILLATION YIELD

In crystalline tetracene an indication regarding the origin of the scintillation can be obtained from a study of the magnetic field effect. If primary singlets are responsible for at least a part of the scintillation, a positive magnetic field effect should be observed at high fields [Fig. 2(a)]. If secondary singlets (due to triplet-exciton fusion) constitute the major contribution to the total scintillation yield, then only a small negative effect ~(−1 to −2)% is expected at magnetic fields $\gtrsim$ 2000 G.

In crystalline anthracene on the other hand, there should be no magnetic field effect on the primary singlets (or only a small positive effect due to hot fission).[27] Secondary singlets created via fusion of triplet excitons should give rise to the characteristic negative magnetic field effect for $\vec{H} \gtrsim 600$ G.

A comparison of the magnetic field dependence of the scintillation of anthracene and tetracene bombarded by α-particles is shown in Fig. 7. The anthracene curve is in agreement with the result of Klein and Voltz.[18] It shows that fusion of triplet excitons is an important mechanism in the production of the scintillation. However, the magnetic

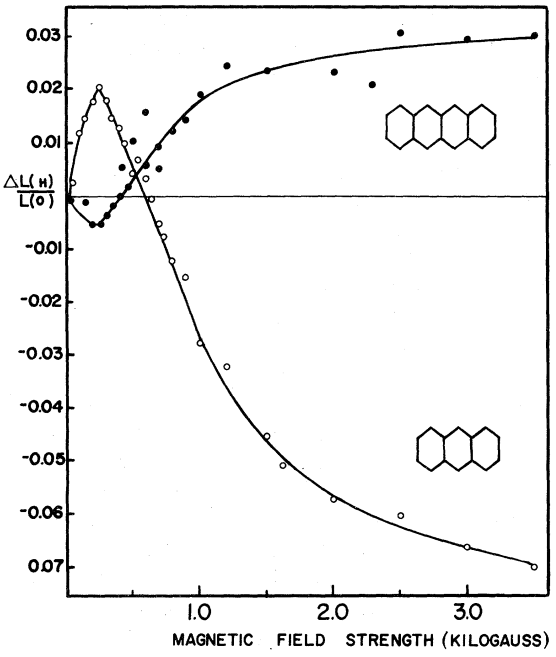

FIG. 7. Magnetic field dependence of the scintillation of tetracene (upper curve), 9-μm-thick flake, ~0.1 cm^2 area, and anthracene (~0.1 cm thick) at (298±1) °K. Magnetic field oriented in the *ab* plane along a resonance direction (see Sec. IV).

field effect close to saturation at 4000 G (not shown in Fig. 7) is only $\sim -7.5\%$, whereas it is about -22% when the external magnetic field is oriented in the *ab* plane on a resonance[55] and when the singlets are generated by fusion only using red light excitation ($T_1 - S_0$).

In tetracene, only the fission of singlet excitons can provide the characteristic positive magnetic effect at high fields with the characteristic inversion at about 430 G. Thus it can be concluded immediately that primary singlets are contributing to the scintillation in tetracene at room temperature. For the crystals studied here, the magnetic field induced enhancement of the prompt fluorescence excited with uv light ($S_1 - S_0$ excitation) was $\sim 35\%$. Thus, the $\sim +3\%$ effect shown in Fig. 7 is much less than in the case of photoexcitation. Using other thicker crystals, the magnetic field effect varied between approximately $+1.5$ and $+2.5\%$, and the average of six crystals was $2.5 \pm 0.5\%$.

The total scintillation is given by Eq. (34) and is a sum of two components: directly generated (L_P) and indirectly generated singlets, the latter giving rise to the delayed component L_D. Of interest is the quenching term γQ_T in Eq. (19) which, using the values of γ in Table I can be used to estimate the effective density of transient quenchers $[Q_T]$ in the α-particle track and thus the singlet-exciton lifetime in the track.

It is evident that γQ_T can be estimated from the magnitude of the magnetic field effect, since k_f, the fission-rate constant which dominates the singlet-exciton lifetime in the absence of quenchers, is known. However, this can be done only if the contribution of the delayed component to the total scintillation can be calculated or can be shown to be negligible at room temperature. If the delayed component L_D is not negligible at 298 °K, the positive magnetic effect which arises from the L_P term in Eq. (34) will be diluted by the magnet-field-insensitive delayed component L_D. Thus, even if $\gamma Q_T \approx 0$, a small magnetic field effect on the total scintillation is expected when $L_D \gg L_P$.

The contribution of the delayed component at room temperature can be estimated by examining the temperature dependence of the total scintillation of tetracene.

VI. TEMPERATURE DEPENDENCE OF THE SCINTILLATION OF TETRACENE AND ITS MAGNETIC FIELD DEPENDENCE

The magnetic field dependence of the scintillation of one and the same crystal at two different temperatures is shown in Fig. 8. At 298 °K the typical fissionlike curve is obtained (compare with Fig. 7). At 148 °K, however, the typical fusion curve is obtained. Below 160 °K, thermally induced fission of singlet excitons is suppressed and consequently the uv-excited ($S_1 - S_0$) prompt fluorescence is not sensitive to magnetic field.[20] On the other hand, delayed fluorescence excited by red light ($T_1 - S_0$) exhibits the type of curve[22] shown in Fig. 8 (148 °K).

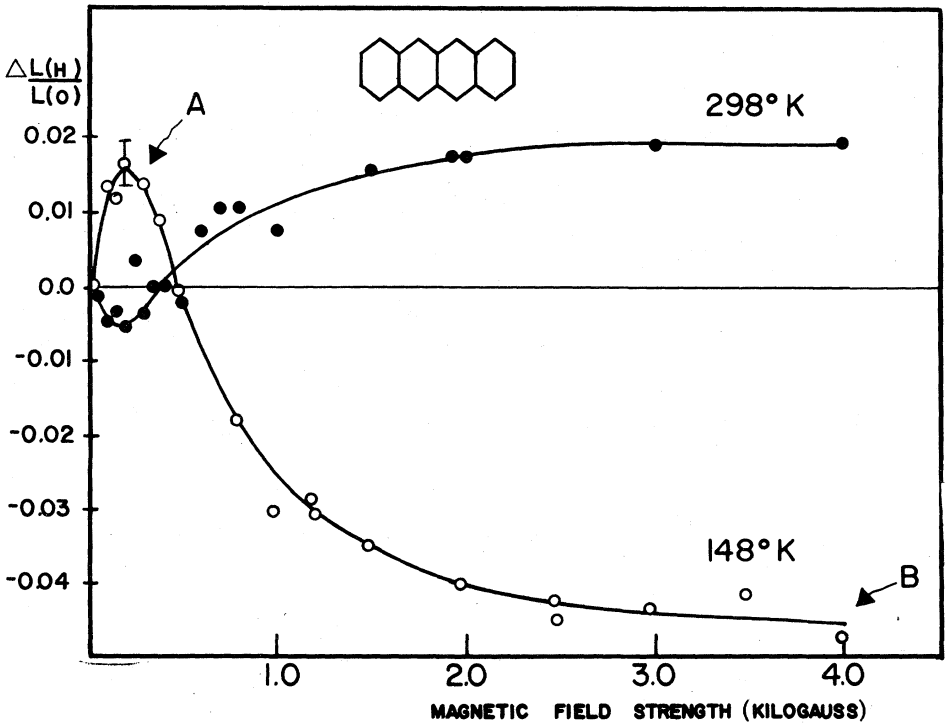

FIG. 8. Effect of magnetic field on the scintillation of tetracene (12 μm thick) at 298 and 148 °K. The contribution of the delayed component L_D to the total scintillation L can be calculated from the value of $\Delta L/L$ either at 200 G (point A) or at saturation at 4000 G (B).

At low temperatures therefore, the magnetic field dependence of the scintillation of tetracene is similar to that of anthracene at room temperature and shows that fusion is an important mechanism of generating singlets at 148 °K.

The temperature dependence of the magnetic field dependence of the total scintillation is shown in Fig. 9(a), curve I. For comparison, a portion of the curve showing the magnetic field effect on the uv-excited prompt fluorescence (photofluorescence) of tetracene is also shown in Fig. 9(a) (curve II). The temperature dependence of the total scintillation $L(\vec{H}=0)$ is shown in Figure 9(b), curve I. Curve II in Figure 9(b) shows the typical temperature dependence of the photofluorescence in the absence of a magnetic field (see Ref. 20).

Writing the explicit temperature dependence of the fission-rate constant as

$$k_f(\vec{H}) = k_0(\vec{H})e^{-\Delta E/kT} \quad , \tag{35}$$

the expression for the prompt scintillation [Eq. (20)] assumes the form

$$L_P(\vec{H}, T) = \frac{k_F N_P}{k_F + k_0(\vec{H})e^{-\Delta E/kT} + \gamma[Q_T]} . \tag{36}$$

We have neglected the term $\gamma[Q_P]$, the quenching of singlet excitons by permanent quenchers, because we are discussing the results obtained with crystals in which $Q_P \ll Q_T$ (low doses of irradiation). Using Eqs. (22), (25), and (33), the delayed component of the scintillation is given by

$$L_D(\vec{H}, T) = \frac{k_F N_T \gamma_{rad}(\vec{H})}{2}\left(\gamma_{tot}(\vec{H}) - \frac{k_0(\vec{H})e^{-\Delta E/kT}\gamma_{rad}(\vec{H})}{k_0(\vec{H})e^{-\Delta E/kT} + k_F + \gamma[Q_T']}\right)^{-1}\{k_0(\vec{H})e^{-\Delta E/kT} + \gamma[Q_T'] + k_F\}^{-1} . \tag{37}$$

In determining $L_D(\vec{H}, T)$ we distinguish a high- and low-temperature limit.

(i) At 298 °K, the high-temperature limit, if the density of quenchers Q_T' is low, we have

$$k_0(\vec{H})e^{-\Delta E/kT} \gg k_F + \gamma[Q_T'] . \tag{38}$$

Under these conditions Eq. (37) reduces to

$$L_D(\vec{H}, T) \doteq \frac{k_F N_T \gamma_{rad}(\vec{H})}{2\gamma_{TT} k_0(\vec{H})e^{-\Delta E/kT}} \quad , \tag{39}$$

where γ_{TT} is the rate constant for the process

$$T_1 + T_1 \rightarrow T_1 + S_0 \quad , \tag{40}$$

i.e., fusion via the triplet channel, γ_{TT}, is known to be magnetic field insensitive.[21] In obtaining Eq. (39) we have used the relationship

$$\gamma_{tot}(\vec{H}) = \gamma_{TT} + \gamma_{rad}(\vec{H}) . \tag{41}$$

It is well known that for the thermal-fission process $k_f(\vec{H})$ and $\gamma_{rad}(\vec{H})$ are related by the thermodynamic relationship[54]

$$k_f(\vec{H})[S_0]^{-1} = \tfrac{9}{2}\gamma_{rad}(\vec{H})e^{-\Delta E/kT} \quad , \tag{42}$$

where $[S_0] = 3.4\times10^{21}$ is the concentration of molecules per cm^3 in crystalline tetracene. Using Eqs. (35) and (42) one obtains for the high-temperature radiative-fusion rate

$$\gamma_{rad}(\vec{H}) = 2k_0(\vec{H})/9[S_0] \quad , \tag{43}$$

which is temperature independent, as long as the temperature dependence of γ_{rad} due to the temperature dependence of the diffusion coefficient D[56] ($\gamma_{rad} \propto D$) is ignored. We are primarily interested in interpreting the temperature dependence of L in the range of 200–300 °K [Fig. 9(b)]. In this temperature range, in anthracene, D increases by not more than[56] (50–60)%, while the scintillation intensity increases by only ~ 25%.[57] In tetracene on the other hand $L(0)$ increases by a factor of four. Furthermore, comparisons with the $L(H)/L(0)$ curve in Fig. 9(a) strongly indicate that this temperature dependence of $L(0)$ in the range of 200–300 °K is due to the magnetic-field-sensitive channel and thus to the strongly varying exponential factor and not to any temperature dependence of D.

Thus, at room temperature, the delayed component L_D should be approximately independent of magnetic field strength, i.e.,

$$L_D(298\,^\circ\mathrm{K}) \approx \frac{k_F N_T e^{\Delta E/kT}}{9\gamma_{TT}[S_0]} \quad \text{(at 298 °K)} . \tag{44}$$

The small negative magnetic field effect in the delayed fluorescence observed by Groff *et al.*[22] is due to the fact that the monomolecular decay term in Eq. (38) is not completely negligible compared to the fission term and thus the magnetic-field-dependent terms in equation (37) do not quite cancel out.

(ii) Low temperatures (below 160 °K, fission is negligible). Under these conditions

$$k_0(\vec{H})e^{-\Delta E/kT} \ll k_F + \gamma[Q_T'] . \tag{45}$$

The delayed fluorescence L_D reduces to the following:

$$L_D(\vec{H}, T) \approx \frac{k_F N_T}{2(k_F + \gamma[Q_T'])} f(H) \quad , \tag{46}$$

where $f(H)$ is the ratio of the radiative- to total-triplet fusion-rate constants, i.e.,

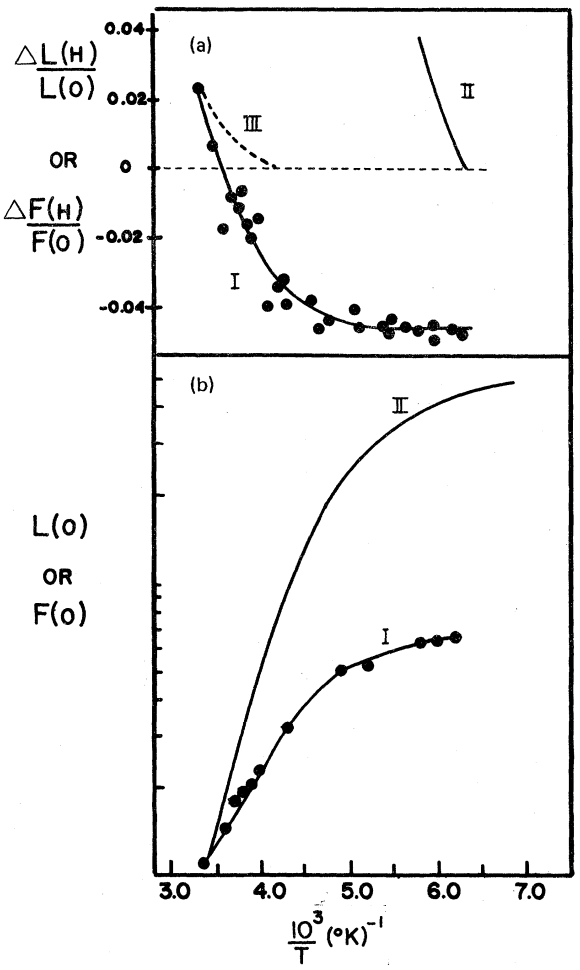

FIG. 9. (a) Temperature dependence of $\Delta L(\vec{H})/L(0)$ in tetracene (28 μm thick). [Effect of magnetic field on the scintillation—curve I; curve II—temperature dependence (Ref. 20) of $F(\vec{H})/F(0)$, where F is the fluorescence intensity excited with uv ($S_1 - S_0$) exciton.] Curve III—calculated temperature dependence of the prompt component ($L_D = 0$ and thus $L = L_P$). (b) Temperature dependence of the fluorescence F (uv excitation) and of the scintillation L excited by α particles.

$$f(\vec{H}) = \gamma_{rad}(\vec{H})/\gamma_{tot}(\vec{H}) \tag{47}$$

and we have set $\gamma_{eff} \approx \gamma_{tot}$.

Equation (46) also applies to the delayed component of the total scintillation from solid anthracene, since in this case thermally induced fission is absent at any temperature.

We note an important fact: The delayed fluorescence is usually excited with red light which is weakly absorbed. The triplet-exciton distribution is therefore homogeneous and under the usual conditions of moderate light intensity the monomolecular decay rate determines the exciton density. Under these conditions the delayed fluorescence is proportional to γ_{rad}. The delayed scintillation component however is proportional to $\gamma_{rad}/\gamma_{tot}$. This is a consequence of the high triplet-exciton densities in the α-particle track (see Sec. II) since the bimolecular decay rate determines the exciton density. In tetracene[30] $f = 0.66 \pm 0.06$ whereas it equals 0.36 ± 0.02 for anthracene.[56] The effect of the high triplet-exciton density gives rise to a reduction of the magnetic field dependence of the delayed scintillation component as compared to that of the photoexcited delayed fluorescence, when the monomolecular decay rate is much larger than the bimolecular decay rate. In the latter case the magnetic-field-induced change is proportional to $\gamma_{rad}(\vec{H})/\gamma_{rad}(0)$, whereas for scintillation it is proportional to $f(\vec{H})/f(0)$. A plot of the relation between $\gamma_{rad}(\vec{H})/\gamma_{rad}(0)$ and $f(\vec{H})/f(0)$ using $f(0) = 0.66$ for tetracene and 0.36 for anthracene is shown in Fig. 10. Using Eq. (41), the equation relating these two quantities can be shown to be equal to

$$\frac{f(\vec{H})}{f(0)} = \frac{\gamma_{rad}(\vec{H})/\gamma_{rad}(0)}{f(0)\{[\gamma_{rad}(\vec{H})/\gamma_{rad}(0)] - 1\} + 1} . \tag{48}$$

The magnetic field effect on the photoexcited delayed fluorescence is equal to $\gamma_{rad}(\vec{H})/\gamma_{rad}(0)$ which, theoretically,[58] can have a lower limit of $\frac{2}{3}$. Experimentally, the maximum ratio for this quantity was observed to be ~ 1.05 [at fields below 200 G, see Fig. 2(b)]. Therefore in Fig. 10, the values

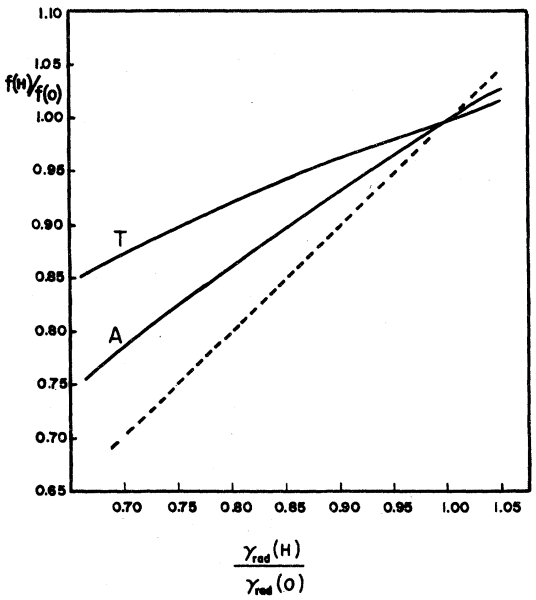

FIG. 10. Plot of $f(\vec{H})/f(0)$ as a function of $\gamma_{rad}(\vec{H})/\gamma_{rad}(0)$ according to Eq. (48) for anthracene [$f(0) = 0.36$] and tetracene [$f(0) = 0.66$]. Owing to the high triplet-exciton densities in the track, the delayed scintillation component L_D is proportional to $f(\vec{H})/f(0)$, rather than to $\gamma_{rad}(\vec{H})/\gamma_{rad}(0)$. See Sec. VI.

of $\gamma_{rad}(\vec{H})/\gamma_{rad}(0)$ have been limited to the range 0.66–1.05.

It is apparant from Fig. 10 that even if the total scintillation was exclusively due to the delayed component ($L = L_D$), the magnetic field effect would be less pronounced than in the photoexcitation case. This effect is more pronounced in tetracene than in anthracene because f is larger in tetracene.

The magnetic field dependence of the total scintillation is

$$\frac{\Delta L(\vec{H})}{L(0)} = \frac{L(\vec{H}) - L(0)}{L(0)} \quad . \tag{49a}$$

In the low-temperature limit (below 160 °K) the fission channel is suppressed and equation (49a) reduces to

$$\frac{\Delta L(\vec{H})}{L(0)} = \frac{L_D(\vec{H}) - L_D(0)}{L_P(0) + L_D(0)} \quad , \tag{49b}$$

where we have used the fact that at low temperatures the prompt component is not magnetic field sensitive. We now let the prompt fluorescence component at low temperatures be larger than the delayed component in zero magnetic field by a factor of X. We write therefore

$$\begin{aligned} L_P(0) &= X L_D(0) \quad , \\ L(0) &= (1+X) L_D(0) \quad , \end{aligned} \tag{50}$$

and

$$\frac{\Delta L(\vec{H})}{L(0)} = (X+1)^{-1}\left(\frac{L_D(\vec{H})}{L_D(0)} - 1\right) \quad . \tag{51}$$

The factor $(X+1)^{-1}$ is a dilution factor as far as the magnetic field effect is concerned: the larger the prompt fluorescence component in the low-temperature limit, the smaller the magnetic field effect. Since $\Delta L(\vec{H})/L(0)$ is measured experimentally and $L_D(\vec{H})$ is given by Eq. (46), the factor X can be estimated under certain conditions. By using Eq. (46) we can rewrite Eq. (51) as

$$\frac{\Delta L(\vec{H})}{L(0)} = (X+1)^{-1}\left(\frac{f(\vec{H})}{f(0)} - 1\right) \quad ; \tag{52}$$

$f(\vec{H})/f(0)$ can be obtained from Fig. 10, since the factor $\gamma_{rad}(\vec{H})/\gamma_{rad}(0)$ is known from photoexcitation studies at the on-resonance orientation of the magnetic field in the *ab* plane which has been the orientation employed throughout these experiments.

In writing Eq. (52), the assumption has been made that any magnetic field dependence of γ can be neglected, which is certainly correct as long as $k_F \gg \gamma([\bar{Q}_T'] + [\bar{Q}_P])$. If γ is magnetic field dependent it is expected to follow the curve shown in Fig. 2(c) as the magnetic field strength is increased. Also, $f(\vec{H})/f(0)$ in Eq. (52) should be multiplied by $\gamma(0)/\gamma(\vec{H})$ if the magnetic field dependence of γ is non-negligible. It will be shown in Sec. IX however that the effect of magnetic field on γ is less than 1%, and therefore does not significantly affect the magnetic field behavior of $\Delta L(\vec{H})/L(0)$. Furthermore, a close examination of the fusionlike curve in Fig. 8 can also offer an indication whether the term $\gamma(0)/\gamma(\vec{H})$ is making a significant contribution to $\Delta L(\vec{H})/L(0)$ or not.

Suppose that $\gamma(0)/\gamma(\vec{H})$ is not negligible. Since $f(\vec{H})$ shows the characteristic low-field inversion, and tends to increase monotonically with increasing field strength, $\Delta L(\vec{H})$ would tend to be larger at point A in Fig. 8, and would tend to be algebraically higher (absolute value smaller) at point B, in the high field limit.

Thus, if X is estimated from Eq. (52) and from the $\Delta L(\vec{H})/L(0)$ value at point B, this calculated value of X will be smaller if the contribution of the term $\gamma(0)/\gamma(\vec{H})$ is *not* negligible. The contribution of the delayed component will then be *underestimated*. If X is estimated from point A, both $f(\vec{H})/f(0)$ and $\gamma(0)/\gamma(\vec{H})$ are greater than unity in this low magnetic field limit, and the value of X will be *overestimated*, thus giving an upper limit for the contribution of the delayed component.

Using these criteria, and the anthracene curve shown in Fig. 7, the delayed component is estimated to contribute between ~ 50 and 70% of the total scintillation in anthracene. This is in good agreement with the results of Bönsch,[59] who showed that at least 50% of the total scintillation of crystalline anthracene is emitted after 50 nsec, whose origin must therefore be from the fusion channel.

In tetracene at A, $f(\vec{H})/f(0) \approx 1.02$ [since $\gamma_{rad}(\vec{H})/\gamma_{rad}(0) \approx 1.05$, see Ref. 22]. However, the value of $f(\vec{H})/f(0)$ at low magnetic fields is sufficiently uncertain, and the scatter in the experimental data is significant enough to preclude any meaningful estimate of X from the $\Delta L(\vec{H})/L(0)$ value at point A in Fig. 8. However, using the value of $\Delta L(\vec{H})/L(0)$ at point B, which yields $\Delta L(\vec{H})/L(0) \cong -0.045$, we estimate that the contribution of the delayed component is ~ 50% at ~ 150 °K.

The upper limit of the contribution of L_D to L [which would be different from the lower limit only if $\gamma(0)/\gamma(\vec{H}) > 1$] cannot be calculated from A as indicated above because of experimental uncertainties involved. However, it can be shown from the field dependence that the effect of $\gamma(0)/\gamma(\vec{H})$ is negligible. The crossover, from the positive to the negative magnetic field region in the fusion curve in tetracene occurs between 420 and 440 G in tetracene. Any sizeable contribution of the quenching-rate-constant factor $\gamma(\vec{H})/\gamma(0)$ would tend to raise the curve numerically and thus shift the crossover point to higher magnetic field strength, as well as increase the numerical value of $\Delta L(\vec{H})/L(0)$ at point A. The crossover of the 148 °K fusion curve (Fig. 8) appears just slightly above the 420–440-

G-photoexcited delayed fluorescence curve crossover. Within the experimental error in Fig. 8 this shift is negligible. We therefore conclude that the contribution of the $\gamma(0)/\gamma(\vec{H})$ term to $\Delta L(\vec{H})/L(0)$ in Eq. (52) can indeed be neglected. The conclusion that in tetracene the contribution of the delayed component to the total scintillation is ~ 50% at low temperatures is thus strengthened.

Using this result, i.e., that $L_D(0) \approx 0.5L$ at 148 °K, together with the temperature dependence of $\Delta L(\vec{H}, T)/L(0)$ and $L(\vec{H}, T)$, the contribution of L_D to the total scintillation at room temperature can be estimated.

We first note that the temperature dependence of the scintillation L is similar to that of the photofluorescence F. However, $F(T)$ changes by a much larger amount than $L(T)$ in the temperature interval shown in Fig. 9. The activation energy for F is ~ 0.20 eV, while it appears to be smaller for L (~ 0.11 eV). This could arise from the fact that the $\gamma[Q]$ term is not negligible relative to the fission term in Eq. (46). This would also lead to a lower value of the quantity $L(160\,°\text{K})/L(298\,°\text{K})$, since the "bend" in the curves in Fig. 9(b) occurs approximately when

$$k_0(\vec{H})e^{-\Delta E/kT} \approx k_F + \gamma[Q]\,. \tag{53}$$

If no fusion were present, $\Delta L(\vec{H})/L(0)$ would remain positive at all temperatures; however, it becomes negative at ~ 0 °C indicating that fusion is contributing more strongly to $\Delta L(\vec{H}, T)/L(0, T)$ as the temperature is lowered. Since the observed $\Delta L(\vec{H}, T)/L(0, T)$ decreases with decreasing temperature (becoming negative below 293 °K) and seems to reach a steady value at a temperature when Eq. (53) is fulfilled approximately [see the bend in I of Fig. 9(b) and compare to I in 9(a)], it appears that most of the temperature dependence in the interval studied is attributable to the fusion process as shown in the delayed fluorescence term $L_D(\vec{H}, T)$. If only fission were operative, then the variation of $\Delta L(\vec{H})/L(0)$ with temperature would be described by curve III in Fig. 9(a). The variation in the photofluorescence efficiency (uv excitation) with magnetic field and temperature is shown in II of Fig. 9(a) for comparison.

The conclusion that the temperature dependence of $L(\vec{H}, T)$ arises mainly from the temperature dependence of $L_D(\vec{H}, T)$ implies that the quenching term due to the transient quenchers is much larger in L_P than in L_D. Thus,

$$\gamma[Q] \gg \gamma[Q']\,. \tag{54}$$

This implies that the prompt scintillation term L_P in Eq. (36) is relatively insensitive to temperature.

Since at 140 °K about 50% of the total scintillation is due to the delayed term, and since the total scintillation decreases by a factor of about 7 ± 1 (the average of three different crystals) as the temperature is increased to 298 °K, we conclude that the contribution of the delayed term at 298 °K to the total scintillation is only 10% or less at 298 °K. At room temperature, therefore, the dominant contribution to L is due to the prompt component, i.e., the primary singlets. This conclusion is further substantiated by the fact that we observe a fission-like magnetic field dependence at 298 °K.

VII. DIFFERENCES IN SCINTILLATION YIELD BETWEEN ANTHRACENE AND TETRACENE

In anthracene at room temperature the contribution of the delayed component is much bigger than in the case of tetracene. The quenching term $\gamma[Q_T]$ which appears in the expression for the prompt scintillation component L_P [Eq. (20)] is due to the transient quenchers. This term appears to be significantly greater than the fission term, since $\Delta L(\vec{H})/L(0)$ at 298 °K in tetracene is only $+2.5 \pm 0.5\%$.

The prompt scintillation component L_P should not be too different in anthracene and tetracene, since the importance of the fission term in the latter is suppressed due to the dominance of the transient-quenching term. Thus, while there is a large difference in the photofluorescence quantum yield in these two crystals, the yield of the prompt scintillation components in these two crystals should be quite similar. The delayed component on the other hand should be much smaller in tetracene. Because of the relatively long time scales when the delayed fluorescence appears (time domain III), the density of transient quenchers is much less than in the short time domain, i.e., $\gamma[Q_T] \gg \gamma[Q_T']$, and fission can now dominate the decay of the singlets.

We measured the relative intensities of several anthracene and tetracene crystal pairs of the same thicknesses. After correcting for the spectral dependence of the photomultiplier sensitivity, we obtained the following ratios of the total scintillation efficiencies at 298 °K:

$$L_{\text{anthracene}}/L_{\text{tetracene}} = 6 \pm 2 \tag{55}$$

(average of eight crystal pairs). This result is consistent with the analysis offered in Sec. VI. Thus, while the photofluorescence efficiency of tetracene at room temperature is at least two orders of magnitude less than that of anthracene, the scintillation efficiencies are not that much different at room temperature.

Lowering the temperature increases the contribution of L_D in tetracene as fission is suppressed. At 150 °K, when thermally induced fission is negligible, $L(150\,°\text{K})/L(298\,°\text{K}) \approx 7$–9 and the total scintillation efficiency and the magnetic field effect on L of anthracene and tetracene become comparable. (There is comparatively little change in the scintillation efficiency of anthracene as the temperature is lowered.)

VIII. CALCULATION OF THE DENSITY OF TRANSIENT QUENCHERS

We have shown that at room temperature the delayed scintillation component contributes less than 10% of the total scintillation. We thus write

$$L(298\,^\circ\mathrm{K}, 0) \approx L_P \tag{56}$$

and using $k_f(0) = 5\times 10^9$ sec^{-1} and Eq. (37) we obtain

$$\frac{\Delta L(\vec{H}, 298\,^\circ\mathrm{K})}{L(0)} \approx 0.025 \pm 0.005 = 1 - \frac{k_f(0)+\gamma[Q_T]}{k_f(\vec{H})+\gamma[Q_T]} \,. \tag{57}$$

The experimental values of Eq. (57) were the results of measurements on six different crystals with thicknesses in the range of 9–30 μm. Since both $k_f(0)$ and $k_f(\vec{H})$ [$= 0.74\, k_f(0)$] for resonance orientations of the external field are known from photofluorescence studies, the quenching term $\gamma[Q_T]$ can be estimated. It is concluded that these quenchers are transient in nature and are effective only in the time domain II for the following reason: the same density of quenchers $[Q_T]$ in Eq. (57) is no longer operative in time domain III, i.e., on time scales when fusion contributes strongly to L. This is evident from the strong temperature dependence of L (which is due to L_D) shown in Fig. 9(b) (curve I), which indicates that the temperature-dependent fission term dominates in the denominator of the L_D term in Eq. (37). This can only be the case if $k_f(\vec{H}, T) > \gamma[Q_T']$, where $[Q_T']$ is the density of quenchers which is operative in time domain III. We therefore also conclude, from the small magnetic field effect on $L(298\,^\circ\mathrm{K}) \approx L_P$, that $[Q_T] \gg [Q_T']$ [see Eq. (54)].

The calculation of $\gamma[Q_T]$ from Eq. (57) yields the following values:

$$\gamma[Q_T] \approx (5 \pm 1)\times 10^{10} \text{ sec}^{-1} \,. \tag{58}$$

Using values of $\gamma \approx 2\times 10^{-7}$–$10^{-8}$ cm^3 sec^{-1} (see Sec. II) which is the estimated rate constant for quenching by either carriers or triplet excitons, we estimate that the effective average density of transient quenchers in the α-particle track is

$$3\times 10^{17} \lesssim [Q_T] \lesssim 5\times 10^{18} \text{ cm}^{-3} \,. \tag{59}$$

This number agrees reasonably well with the density of free carriers and triplet excitons in this time domain estimated in Sec. II. We note that in anthracene, the singlet lifetime in the absence of quenchers is ~ 20 nsec and therefore much longer than in tetracene. Furthermore, the diffusion of excitons is much smaller in anthracene which extends time domain II as shown in Fig. 4 to longer time scales. For these reasons, in anthracene the triplet excitons, whose density remains fairly constant in time domain II, are expected to be more effective quenchers than the free carriers, whose density diminishes rapidly with increasing time in domain II. This agrees with the conclusions of Schott.[12] In tetracene, the quenching by free carriers is probably more important than in anthracene, although this conclusion is only a hypothesis at this time.

From Eq. (58) we estimate that the singlet-exciton lifetime in the α-particle track in time domain II is of the order of $\sim 2\times 10^{-11}$ sec.

In summary, the validity of the calculation of the concentration of transient quenchers rests on the following conditions: (i) The contribution of the delayed component to the total scintillation at room temperature can be neglected as has been indicated, (ii) the singlet-exciton quenching constants γ are themselves not magnetic field sensitive (true if the quenchers $[Q_T]$ are triplets, and unknown if $[Q_T]$ are mostly free carriers), and (iii) the magnitude of the quenching constants γ for S-T quenching and S-n^* quenching are correct within the limits of 10^{-7}–10^{-8} cm^3 sec^{-1} in the α-particle tracks.

IX. EFFECTS OF PROLONGED IRRADIATION

If the tetracene crystal is exposed to the α particle for a prolonged period of time, both the scintillation efficiency L and the photofluorescence F (excited with near-uv light) decrease with time. Prior to the irradiation, a magnetic field of ~ 4000 G results in a ~ 35% increase in F at room temperature. With increasing time of exposure the ratio $F(\vec{H})/F(0)$ decreases gradually and can drop from its initial value of 1.35 to a value of as low as 1.04 after being exposed to a total of 10^{11} α-particles/cm^2 (~ 10^6 rad). This result indicates that long-lived or permanent singlet-exciton quenching centers are formed (denoted by Q_P in previous sections). This decrease implies that the density $[Q_P]$ of these quenchers is sufficiently high so that the quenching rate constant $k_Q = \gamma Q_P$ is of the same order of magnitude or larger than the fission rate constant k_f. The magnetic field effect on the photofluorescence efficiency F is given by

$$\frac{F(\vec{H})}{F(0)} = \frac{k_f(0)+k_Q(0)}{k_f(\vec{H})+k_Q(\vec{H})} \tag{60}$$

at room temperature. As k_Q increases, the $F(\vec{H})/F(0)$ ratio decreases. We have established that $k_Q(0)/k_Q(\vec{H}) \approx 1.0$ by noting that there was no field effect on F ($\lesssim \pm 1\%$) at low temperature (~ 150 °K) in a highly irradiated crystal where $k_Q \gg k_f$. Thus k_Q can in principle be calculated from Eq. (60) and the experimentally determined values of $F(\vec{H})/F(0)$. However, the penetration depth of the light used in such studies typically has absorption depths of several microns at the most, with the largest fraction of the light absorbed near the illuminated surface according to Beer's law. In the case of an α particle, however, the well-known Bragg curve describes the amount of energy deposited as a func-

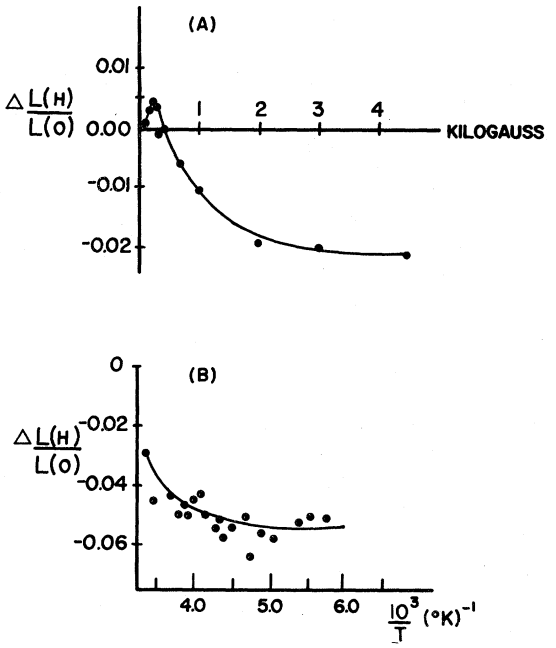

FIG. 11. (a) Effect of magnetic field on the scintillation of a highly irradiated (10^6 rad) tetracene crystal at 298 °K (crystal thickness: 22 μm). (b) Temperature dependence of $\Delta L(\vec{H})/L(0)$ of the same crystal.

tion of the penetration depth. In the region near the surface of the crystal where the density of quenchers is probed by the light, the energy loss by the α particle is comparatively small and reaches a maximum, the Bragg peak, near the end of the trajectory (about 30 μm).

The effect of magnetic field on the total scintillation yield before prolonged irradiation is ~ + (2–3)% at room temperature. Upon prolonged exposure to α particles at room temperature $\Delta L(\vec{H})/L(0)$ continues to decrease with increasing dosage finally approaching the limiting value of about 0.98 at a dosage of 10^6 rad. Initially, $L(\vec{H})/L(0)$ as a function of $\vec{H}$ displays the typical fissionlike curves shown in Figs. 7 and 8 (at 298 °K). After receiving a dosage of 10^6 rad however, the fusionlike curve shown in Fig. 11(a) is obtained. It should be noted that the delayed fluorescence due to photoexcitation, and originating from triplet-exciton fusion, does not display the magnetic field dependence[22] shown in Fig. 11(a) [cf. Fig. 2(b)]. The appearance of permanent quenching centers changes the fissionlike curve obtained before irradiation to a fusionlike curve. This can be understood as follows: In photoexcited delayed fluorescence in tetracene at room temperature, singlet excitons which are formed by fusion of two triplet excitons decay back to two triplets via fission. This results in a cancellation of magnetic field effects since both the fission- and fusion-rate constants are decreased at fields above 500 G.

In the presence of a large density of quenchers however, fission may no longer be the dominant decay channel of singlets which are formed by fusion. Since the quenching itself is not magnetic field dependent, the fusionlike curve will be observed as is the case in Fig. 11(a). The temperature dependence of $L(\vec{H})/L(0)$ is shown in Fig. 11(b). It is seen to decrease from a value of ~ 2.5% at room temperature to ~ – 5.5% in the low-temperature limit. The temperature dependence of the total scintillation is also much weaker in the case of the highly irradiated crystal. Thus, between 298 and 220 °K, $L(0)$ rises by a factor of 4 (Fig. 9) but rises by only a factor of 2 in the case of highly irradiated (10^6 rad) crystals [for which the magnetic field dependence of L is shown in Fig. 11(a)].

These results are in general agreement with the previous analysis. The permanent quenchers which are introduced tend to develop a fusionlike magnetic field dependence in the delayed scintillation term L_D at room temperature. The magnitude of the prompt scintillation term L_P is reduced in intensity by the introduction of the permanent quenchers. Therefore, the positive magnetic field dependence contributed by the L_P term is decreased, while a negative contribution due to the L_D term appears. In the highly irradiated crystal, one can conclude from Fig. 11(a) that

$$\left|\frac{\Delta L_D(\vec{H})}{L_D(0)}\right| > \left|\frac{\Delta L_P(\vec{H})}{L_P(0)}\right|$$

at 298 °K, whereas exactly the opposite is true prior to irradiation. After receiving a dosage of 10^6 rad, the relative total scintillation is only ~ 20% of its original value. It can be shown[60] that this corresponds to the introduction of about $\sim 10^{18}$ quenching centers per cm^{-3}. Using this value of $[Q_P]$ and $\gamma \approx 10^{-7}$ cm^3 sec^{-1} for quenching of singlets by carriers (it will be similar for trapped carriers, radicals, or impurities), we obtain $k_Q \approx 10^{11}$ sec^{-1}, which is sufficiently large compared to the fission rate of $k_f \approx 5 \times 10^9$ sec^{-1}, to account for the observations shown in Fig. 11. We also note that a concentration of 10^{18} cm^{-3} of radiation-induced quenching centers is not unusual in organic crystals.[61,62]

ACKNOWLEDGMENTS

This work was supported by the Atomic Energy Commission. We would like to thank W. Bizzarro and J. B. Tinkel for their assistance in the initial phases of this work. One of us (C.E.S.) wishes to thank Dr. J. B. Birks for his hospitality during his visit at the Schuster Laboratory at the University of Manchester and for stimulating discussions.

[1]J. B. Birks, *The Theory and Practice of Scintillation Counting* (Pergamon, Oxford, 1964).
[2]J. B. Birks, Proc. Phys. Soc. Lond. A 64, 874 (1951).
[3]G. T. Wright, Phys. Rev. 91, 1282 (1953).
[4]R. Voltz, J. Lopes da Silva, G. Laustriat, and A. Coche, J. Chem. Phys. 45, 3306 (1966).
[5]T. A. King and R. Voltz, Proc. R. Soc. A 289, 424 (1966).
[6]P. H. Heckmann, Z. Phys. 157, 139 (1959).
[7]W. F. Kienzle and A. Flammersfeld, Z. Phys. 165, 1 (1964).
[8]W. F. Kienzle, Z. Naturforsch A 19, 756 (1964).
[9]F. J. Kratochwill, Z. Phys. 234, 74 (1970).
[10]K. Wille, Z. Phys. 241, 55 (1971).
[11]R. Voltz, in *International Discussion on Progress and Problems in Contemporary Radiation Chemistry* (Academia, Prague, 1971), Vol. 1, p. 139.
[12]M. Schott, thesis (Université de Paris, 1972) (unpublished).
[13]P. Avakian and R. E. Merrifield, Mol. Cryst. Liq. Cryst. 5, 37 (1968).
[14]R. E. Merrifield, Pure Appl. Chem. 27, 481 (1971).
[15]P. Avakian, Pure Appl. Chem. 37, 1 (1974).
[16]C. E. Swenberg and N. E. Geacintov, in *Organic Molecular Photophysics*, edited by J. B. Birks (Wiley, New York, 1973), Vol. 1, Chap. 10.
[17]I. A. Sokolik and E. L. Frankevich, Usp. Fiz. Nauk 111, 261 (1973) [Sov. Phys.-Usp. 16, 687 (1974)].
[18]G. Klein and R. Voltz, (private communication) and Sixth Molecular Crystal Symposium, Elmau, 1973 (unpublished).
[19]W. Bizzaro, N. E. Geacintov, C. E. Swenberg, and M. Pope, Bull. Am. Phys. Soc. 18, 92 (1973).
[20]N. E. Geacintov, M. Pope, and F. Vogel, Phys. Rev. Lett. 22, 593 (1969).
[21]M. Pope, N. E. Geacintov, and F. Vogel, Mol. Cryst. Liq. Cryst. 6, 83 (1969).
[22]R. P. Groff, P. Avakian, and R. E. Merrifield, Phys. Rev. B 1, 815 (1970).
[23]A. W. Smith and C. Weiss, Chem. Phys. Lett. 14, 507 (1972).
[24]R. R. Alfano, S. A. Shapiro, and M. Pope, Opt. Commun. 9, 388 (1973).
[25]E. J. Bowen, E. Mikiewicz, and F. W. Smith, Proc. Phys. Soc. Lond. A 62, 26 (1949).
[26]F. Vogel, Ph. D. thesis (New York University, 1971) (unpublished).
[27]G. Klein, R. Voltz, and M. Schott, Chem. Phys. Lett. 16, 3406 (1972); 19, 391 (1973).
[28]R. E. Merrifield, J. Chem. Phys. 48, 4318 (1968).
[29]N. E. Geacintov and C. Strom (unpublished results).
[30]V. Ern, J. L. Saint-Clair, M. Schott, and G. Delacote, Chem. Phys. Lett. 10, 287 (1971).
[31]T. S. Rahman and R. S. Knox, Phys. Status Solidi B 58, 715 (1973).
[32]J. Fourny, M. Schott, and G. Delacote, Chem. Phys. Lett. 20, 559 (1973).
[33]V. Ern and R. E. Merrifield, Phys. Rev. Lett. 21, 609 (1968).
[34]N. E. Geacintov, M. Pope, and S. J. Fox, J. Phys. Chem. Solids 31, 1375 (1970).
[35]V. Ern and A. R. McGhie, Mol. Cryst. Liq. Cryst. 15, 277 (1971).
[36]V. Ern, H. Bouchriha, J. Fourny, and G. Delacote, Solid State Commun. 9, 1201 (1971).
[37]J. Levinson, S. Z. Weisz, A. Cobas, and A. Rolon, J. Chem. Phys. 52, 2794 (1970).
[38]N. Wakayama and D. F. Williams, J. Chem. Phys. 57, 1770 (1972).
[39]E. L. Frankevich, I. A. Sokolik, and L. V. Lukin, Phys. Status Solidi 54, 61 (1972).
[40]M. Schott and J. Berrehar, Mol. Cryst. Liq. Cryst. 20, 13 (1973).
[41]L. Peter and G. Vaubel, Phys. Status Solidi B 48, 587 (1971).
[42]M. Silver and R. Sharma, J. Chem. Phys. 46, 692 (1967).
[43]G. E. Heppell, J. Chem. Phys. 41, 577 (1964).
[44]H. Ehrhardt and F. Linden, Z. Naturforsch. A 22, 444 (1967).
[45]I. Santar and J. Bednar, Collect Czech. Chem. Commun. 34, 1 (1969).
[46]W. P. Jesse, J. Chem. Phys. 41, 2060 (1964).
[47]W. G. Perkins, J. Chem. Phys. 48, 931 (1968).
[48]D. C. Northrop and O. Simpson, Proc. R. Soc. A 234, 136 (1956).
[49]G. T. Pott and D. F. Williams, J. Chem. Phys. 51, 203 (1971).
[50]V. Ern, Phys. Rev. Lett. 22, 343 (1969).
[51]R. Voltz, H. Dupont, and G. Laustriat, J. Phys. 29, 297 (1968).
[52]R. Voltz and G. Laustriat, J. Phys. 29, 159 (1968).
[53]R. P. Groff, R. E. Merrifield, and P. Avakian, Chem. Phys. Lett. 5, 168 (1970).
[54]R. E. Merrifield, P. Avakian, and R. F. Groff, Chem. Phys. Lett. 3, 155 (1969).
[55]R. P. Groff, R. E. Merrifield, P. Avakian, and Y. Tomkiewicz, Phys. Rev. Lett. 25, 105 (1970).
[56]V. Ern, A. Suna, Y. Tomkiewicz, P. Avakian, and R. P. Groff, Phys. Rev. B 5, 3222 (1972).
[57]H. W. Schiffer, Z. Phys. 227, 482 (1969).
[58]W. T. Stacy, T. Mar, C. E. Swenberg, and Govindjee, Photochem. Photobiol. 14, 197 (1971).
[59]G. Bönsch, Z. Phys. 212, 497 (1968).
[60]N. E. Geacintov, M. Binder, C. E. Swenberg, and M. Pope (unpublished).
[61]H. Ringle, W. B. Whitten, and A. C. Damask, Mol. Cryst. Liq. Cryst. 6, 435 (1970).
[62]A. R. McGhie, H. Blum, and M. M. Labes, Mol. Cryst. Liq. Cryst. 5, 245 (1969).